Journal of Urban Economics 143 (2024) 103685

Contents lists available at ScienceDirect

Journal of Urban Economics

journal homepage: www.elsevier.com/locate/jue

Cities and the sea level☆

Yatang Lin[a], Thomas K.J. McDermott[b], Guy Michaels[c,*]

[a] Hong Kong University of Science and Technology, The Hong Kong Special Administrative Region of China
[b] University of Galway, The Republic of Ireland
[c] London School of Economics, The United Kingdom of Great Britain and Northern Ireland

ARTICLE INFO

Dataset link: https://data.mendeley.com/datasets/2jrct63w2t/2

JEL classification:
R11
Q54
R14

Keywords:
Cities
Climate change
Sea level rise

ABSTRACT

Construction on low elevation coastal zones is risky for both residents and taxpayers who bail them out. To investigate this construction, we analyze spatially disaggregated data covering the entire US Atlantic and Gulf coasts. We find that the 1990 housing stock reflects historical avoidance of locations prone to sea level rise (SLR) and flooding, but net new construction from 1990–2010 was similar in SLR-prone locations and safer ones; and within densely built coastal areas, net new construction was higher in SLR-prone locations. These findings are difficult to rationalize as mere products of moral hazard or imperfect information, suggesting that people build on risky locations to benefit from nearby urban agglomerations. To explain our findings, we develop a simple model of a monocentric coastal city, which we use to explore the consequences of sea level rise. This model helps explain cities' role in expanding flood risks, and how future sea level rise may reshape coastal cities, creating significant challenges for policymakers.

1. Introduction

Low Elevation Coastal Zones (LECZ) are attractive places to live. In 2000 they were home to around 10% of the world's population, a figure expected to grow significantly by 2050.[1] But this growing attraction of LECZ poses challenges, as some of their terrain is susceptible to floods. The problem of flooding is expected to worsen as glaciers melt and the oceans warm and expand due to climate change. The UN's Intergovernmental Panel on Climate Change, IPCC (Pörtner et al., 2019), forecasts that mean global sea levels will rise by 43–84 centimeters by 2100. Sea level rise (SLR) is affecting some LECZ more than others, and the US Atlantic and Gulf coasts suffer from some of the fastest rates of local SLR in the world (Dahl et al., 2017). Along with SLR, climate change may also increase the severity of tropical storms (Berardelli, 2019), whose impact is already acutely felt in the US. Since 2005, the US has suffered 173 major weather and climate disasters, most of which were caused by tropical storms, other severe storms, and flooding (NOAA, 2021a).

The severity of major flooding events, such as tropical storms, creates an important role for the government, which deals with catastrophic events that private markets do not fully insure (e.g., CBO (2017), Pralle (2019), and Bakkensen and Barrage, 2021). Recent government estimates suggest that roughly a third of the annual costs imposed by tropical storms in the US is accounted for by public funds (CBO 2019), with taxpayers' burden further increased by the costs of social insurance responses to storms (Deryugina, 2017). And the costs of flooding are rising over time. For example, overall payouts on the National Flood Insurance Program (NFIP) have increased at a rate of roughly 4% per year in real terms since the 1970s, while a series of official reports have highlighted a widening gap between claims and premia.[2]

☆ We thank Juan Alvarez-Vilanova and Tiernan Evans for excellent research assistance. We thank Emek Basker, Tim Besley, David Castells-Quintana, Peter Christensen, Vernon Henderson, Alan Manning, Henry Overman, Steve Pischke, Eric Strobl, and John Van Reenen, and seminar/conference participants at Bank of Spain, CERIS Workshop Galway 2023, CESifo Area Conference on Global Economy, ERSA 2018, Federal Reserve Bank of Philadelphia, IFAU, IZA, LSE, NUI Galway, Queen Mary University of London, UEA North America Meetings 2022, University of Kent, UAB, UCSB, University of Stockholm, Universitat Pompeu Fabra, and the US Census Bureau for their helpful comments. We are grateful to the Hong Kong University Grant Committee, Irish Research Council award no. GOIPD/2017/1147, and the ESRC's Centre for Economic Performance for their generous financial support.

* Corresponding author.
E-mail address: g.michaels@lse.ac.uk (G. Michaels).

[1] These estimates are from Neumann et al. (2015), who refer to LECZ as the contiguous and hydrologically connected zone of land along the coast and below 10 m of elevation. The coastal areas we study are generally low-elevation and close to the coast, as we define and discuss in Section 2.

[2] Estimates of NFIP cost growth are by the authors, described in detail in Appendix B. The widening gap between claims and premia are discussed, for example, in CBO (2017, 2019) and Bakkensen and Barrage (2021).

https://doi.org/10.1016/j.jue.2024.103685
Received 10 March 2023; Received in revised form 3 July 2024
Available online 1 August 2024

Since both residents and taxpayers are exposed to rising flood risk, our paper asks: does new coastal construction avoid risky locations? To study whether this is the case, we use up-to-date high-resolution maps (NOAA, 2021b), which identify SLR-proneness consistently, using a fine vertical and spatial breakdown.[3] This lets us pinpoint locations that will be under water at high tide if sea levels rise by 1 foot, or approximately 30.5 cm, and are even today highly prone to flooding (Dahl et al., 2017 suggest that many areas on US Atlantic and Gulf coasts could experience 1ft SLR as early as 2045). To measure outcomes, we use data on housing units from the Census and American Community Survey from 1990–2010; specifically, we use the finest level of census data available — census blocks. By virtue of their small size, these blocks allow us to identify housing that is at risk of SLR in ways that are impossible using coarser data, such as for counties.

These data reveal two new stylized facts. First, while the density of coastal construction up to 1990 was negatively correlated with SLR (and flood) risk, construction from 1990–2010 was, on average, uncorrelated with such risk. Quantitatively, in 1990, 12% of the coastal housing stock was in blocks prone to one-foot sea level rise. But for (net) new housing built from 1990–2010, this share was 26%, bringing the share of the stock in 2010 to 14%. Second, in areas that were sparsely built in 1990, net new construction from 1990–2010 still avoided SLR-prone locations; but in areas that were densely built in 1990, net new construction was positively correlated with SLR risk. We note however, that even within the densest census tracts, new construction focused on medium-risk SLR-prone areas, still avoiding the riskiest ones.

To paint a richer picture of coastal construction, we use cross-sectional data from around 1990 to show four auxiliary findings. First, housing unit density peaks near – but not right at – the coast, and it declines more steeply on the coast side. Second, census-designated places near the coast are asymmetric – their Central Business District (CBD) is closer to their coast side edge – while places further inland are symmetric. Third, the asymmetry near the coast is more pronounced for large places. Fourth, census blocks that are prone to SLR are much more sparsely built; but conditional on SLR-proneness, blocks closer to the coast are more densely built.[4] Our empirical findings are robust to controlling for Core-Based Statistical Area (CBSA) fixed effects, which address potential concerns about variation in local sea level rise and zoning regulations. They are also robust to controlling for distance to the coast (except where that distance is the main variable of interest) and to excluding census blocks, which were mostly shielded from private residential construction, because they are either protected areas, military bases, or parks. We find very similar patterns using satellite-derived data on built area, which cover all types of construction rather than just housing.

Our empirical findings are difficult to reconcile using only the two common explanations for building on flood-prone areas: moral hazard due to government subsidy, or imperfect information (or understanding). These factors may be important, but they do not explain why SLR-prone areas are typically avoided and built on only when land is scarce. Our findings suggest that a third and previously unexplored mechanism is at work: people build on SLR-prone coastal locations to benefit from nearby urban agglomerations.

To account for our empirical findings, we develop a simple model of a monocentric coastal city. In the model, coastal areas are characterized by both an amenity, which declines linearly in the distance to the coast, and a disamenity (flood-proneness), which declines convexly in distance to the coast.[5] The city founder chooses a location that trades off these two factors – close to the coast, but not right at it. This location becomes the city's focal point – the Central Business District (CBD).[6] Residents then choose where to live, and they prefer locations close to the CBD, both because of their high net amenity value and because of the shorter commute. Housing density peaks around the CBD, but declines more steeply on the coast-side, because of the convex flood-proneness. The city expands over time into previously empty areas on both sides. On the coast side, this expansion involves building on increasingly flood-prone land.

After explaining how our empirical observations are accounted for in the model, we extend the model in several ways. Our first extension allows for sea level rise. The second allows for a limited set of high-elevation locations near the coast, which are safe from flooding and command high prices. Third, we allow for costly and irreversible conversion of land to housing from alternative uses, which makes the developers' decisions dynamic rather than static. Fourth, we examine government subsidies to flood-prone areas. Fifth, we consider the possibility that employment is spread across the city, rather than being concentrated solely in the CBD. Finally, we consider the impact of land use regulations.

We then simulate our model to explore challenges that low-elevation coastal cities may face in the coming decades. These simulations point to four potential concerns for low-elevation coastal cities. First, the problem of housing in flood-prone locations looks set to worsen, either because cities expand towards the coast, or because of SLR, or because both happen simultaneously. This development threatens to increase flooding costs for both residents and taxpayers. Second, even if LECZ cities grow on aggregate, some neighborhoods within them may experience economic decline, as increased flood risk causes demand for housing to decline. This problem is exacerbated in the case of economically stagnant cities. Third, SLR imposes additional costs beyond increased flood risk, by further distorting the shape of LECZ cities, which significantly lengthens the time costs of commuting to work. Finally, these cities face a potential crisis if their CBD comes under threat of being permanently submerged.

We view our model primarily as a qualitative tool for evaluating coastal development. Our model considers a relatively benign case, where people correctly anticipate events and have time to adapt the city gradually. Further, the model does not consider idiosyncratic conditions, which specific cities may face. With these caveats in mind, our welfare analysis sheds light on the costs of sea level rise and of government subsidies to SLR-prone areas, both of which concentrate in the 1 km closest to the coast. At the same time, we find that path dependence in the precise location of the CBD entails relatively lower costs, at least as long as the CBD is not submerged.

The main contributions of our paper are threefold. First, we assemble a new dataset on the location of housing and flood risk, which covers thousands of kilometers of coast, spanning major urban centers, small towns, and rural areas. The data, which cover two decades, are at a highly disaggregated spatial scale. They include information on housing from the census and land cover from satellite imagery, as well as measures of SLR-proneness, flood damages, and regulatory restrictions. These data allow us to explore construction in areas where flood risks for residents and taxpayers are both high and rising, due to climate change. Second, we use these data to study the distribution of the coastal housing stock and show that new construction in recent

[3] In contrast, commonly used data from Federal Emergency Management Agency were not consistently updated across areas. They also identify locations as prone to "1 in T years flood", which is harder to interpret, especially with climate change.

[4] In a related study, Wing et al. (2018) use a flood hazard model to study changing flood risk at a disaggregated spatial level.

[5] Our paper is related to the literature on the importance of urban amenities (Glaeser et al., 2001) and the attraction of coastal areas (Rappaport and Sachs, 2003).

[6] The dynamics we study, where a city forms around a historically determined location, which remains a focal point even when fundamentals change, echoes the findings of Bleakley and Lin (2012) on path-dependent city locations.

decades focused in SLR-prone areas, especially near densely populated areas. Our findings are novel and policy relevant. Finally, we develop a simple model, which provides a parsimonious explanation for our findings. We extend this model and use it to study how SLR may reshape coastal cities and consider the costs of SLR and subsidies for construction in SLR-prone coastal areas.

The literature on flood risk and housing markets has tended to concentrate on estimating price effects for properties exposed to flood risk (for a review see Beltran et al., 2018). Relatively less attention has been paid to quantities, and most previous empirical studies of exposure to SLR risk have tended to be coarser in their spatial resolution (e.g., Burby, 2001; Brody et al., 2007; Dinan, 2017). In recent work, Barrage and Furst (2019) analyze the relationship between new housing additions and exposure to sea level rise for US coastal counties. Our empirical analysis takes a much more fine-grained view, enabling us to present a more nuanced picture of how exposure to flood risk is evolving along the US Atlantic and Gulf coasts. A related literature focuses on policy aspects of managing flood risk, including the relationship between land-use, regulation, and damages from flooding (e.g., Kousky et al., 2013; Taylor and Druckenmiller, 2022), as well as institutional aspects of flood insurance in the US (e.g., Kriesel and Landry, 2004; Michel-Kerjan, 2010; Kousky and Michel-Kerjan, 2017).

Though attractive, LECZ are also prone to flooding, and there are reasons to worry that they might be built over too densely. First, the flood-proneness of LECZ creates moral hazard, which results in overbuilding when taxpayers bear some of the costs of reconstruction following floods (Kydland and Prescott, 1977) and of public construction of flood defenses. Second, flood risk may be under-appreciated by residents because official flood maps do not fully reflect current and future risks (US Department of Homeland Security, Office of Inspector General, 2017), or because people are myopic (Burningham et al., 2008 and Pryce et al., 2011).[7] Our paper posits a third reason why people build in flood-prone coastal areas: to reduce commuting costs to jobs in major city centers, which are often near the coast.

Our paper is also related to the literature on physical barriers to city growth. Building on Saiz (2010), who studies "hard" physical barriers to city growth, we characterize "soft" barriers, such as flood-prone areas (in other contexts, different environmental hazards, such as areas prone to wildfires, may play a similar role). Soft barriers are locations that are not used for housing development in most circumstances but are nevertheless built on as cities expand. Construction on soft barriers may involve risks not only to residents but also externalities (e.g., for taxpayers or the environment), which may necessitate policy intervention. Also closely related is Harari (2020), who studies how physical barriers distort the shape of cities and lengthen commutes. Our paper differs in its geographic focus (the US as opposed to India), and more importantly in its study of flooding and SLR, which further distorts the shape of coastal cities. Another related paper is Magontier et al. (2019), who study the political economy of coastal destruction in Spain. We differ in our focus on market forces (rather than the political economy), and in our study of the role of SLR.

A recent literature quantifies the economic cost of climate change using structural models. For example, Balboni (2020) studies exposure of Vietnam roads to SLR and finds that infrastructure investments that ignore future SLR risks might lead to inefficient persistence in coastal cities, and Desmet et al. (2021) use a spatially disaggregated, dynamic model of the world economy to quantify the roles of migration and local agglomeration for population dynamics and SLR cost. While our model is more stylized, it opens a window into the previously unexplored internal structure of coastal cities and their adjustment to climate change, offering a parsimonious explanation for our novel findings.

[7] Ortega et al. (2018), Gibson and Mullins (2020), Hino and Burke (2020), and Keys and Mulder (2020) explore the updating of house prices following information on flooding and SLR.

Finally, our paper is also related to the literature on the adaptation of cities to large-scale environmental shocks, such as Hornbeck and Keniston (2017) and Kocornik-Mina et al. (2020). Our contribution here is to explore how coastal cities evolve and how SLR reshapes them.

2. Data

2.1. The area and units of analysis

In our analysis we focus on areas within 10 km of the US Atlantic and Gulf coasts. This choice of area reflects a tradeoff between our focus on flood-prone and SLR-prone LECZ and the analysis of fine spatial units. First, we are interested in low-elevation coastal zones, and especially those that are prone to flooding and vulnerable to sea level rise. The area that we study spans the coastal edges of the Atlantic Coastal Plain and the Gulf Coastal Plain, both of which include many low-elevation coastal locations. The area that we study is highly prone to flooding: it held 1.7 percent of US housing units in 1990 (and about 2 percent in 2010) but accounted for 36 percent of the value of National Flood Insurance Program (NFIP) claims from 1973–2019. This area also experienced some of the fastest rates of local sea level rise in the world during the 20th century, a trend which is expected to continue and raise the frequency and severity of floods in these locations (Dahl et al., 2017).

Second, we analyze small spatial units, where the intersection of flood-proneness and construction can be pinpointed. Much of our analysis is at the level of census blocks — the smallest geographic units used by the US Census Bureau. We complement our census block data with a gridded dataset of 150 m × 150 m cells, which is the approximate size of the median census block. More details on this alternative dataset are included below and in the Data Appendix. We also make use of more aggregated geographic units, including census-designated places (administrative cities or towns, which may make up part of a metropolitan area), and census tracts (the finest disaggregation for which we have data on damages from floods from the National Flood Insurance Program). The blocks and other geographical units that we use are from the 1990 census, with later data matched onto them, as detailed below and in the Data Appendix. All the census datasets that we use are sourced from the NHGIS data archive (Manson et al., 2019).[8]

Since, as we discuss below, SLR-prone land and NFIP damages are heavily concentrated within one or two km of the coast, we decided not to explore the area further inland than 10 km.[9] A map of the area that we study is shown in Appendix Figure A1.[10] Since the coast is not straight but winding, the area within 0–1 km of the coast is larger than the area within 1–2 km of the coast, and so on. In our analysis we take this into account, as we explain below.

[8] To characterize the shape of coastal construction, we also obtain data on census-designated places (Manson et al., 2019). These data are useful because they show not only the outline of places, but also (unlike metropolitan areas) their historical CBDs. We use these to calculate place asymmetry, as explained in the Data Appendix.

[9] The only exceptions where we show areas further inland than 10 km are in a few illustrative examples in our appendix, as discussed below. Our economic analysis consistently focuses on the area within 10 km of the coast.

[10] We use the Database of Global Administrative Boundaries (GADM, 2018) to define the coast. This shapefile includes sections of major rivers, such as the Charles in Boston, East River and the Hudson River in New York City, and the Potomac in Washington, DC, as part of the coastline. But lakes and upstream sections of rivers are typically excluded from the coast shapefile, and consequently Philadelphia, New Orleans, and Houston, are largely outside our dataset. Overall, the area we study consists of parts of 18 states and the District of Columbia, as listed in the Data Appendix.

2.2. Housing and land cover data

Our housing data come from the US Census and American Community Survey, observed in 1990 and 2010, which cover all housing unit types.[11] We harmonize all our census data to the geographical units (block boundaries) of the 1990 census, with 2010 data matched to 1990 in proportion to area shares, as described in detail in the Data Appendix. Our main dataset, composed of census blocks within 10 km of the US Atlantic and Gulf coasts, includes some 544,071 observations, covering a total area of 128,757 sq km. The median area of blocks in our data is 0.021 sq km (like a square with 145 meters on each side), and the median number of housing units per block in 1990 is 12. At the level of blocks, we observe the number of housing units and the median price of owner-occupied dwellings (housing units).[12] We complement the housing quantity data with house price data from the census, as we discuss in the appendix.

As an alternative measure of the extent and intensity of development in coastal areas, we use land cover data based on Landsat Thematic Mapper (TM) satellite imagery (NOAA, 2021c). The Landsat data come in the form of a raster dataset where each 30 m × 30 m observation (or pixel) has been assigned to one of 25 land cover categories.[13] In our analysis, we focus on the four developed categories, which represent different extents of constructed surfaces (including buildings, roads, and parking lots).[14] We aggregate the Landsat data to 150 m × 150 m cells (the approximate size of the median census block in our data), taking the midpoint values of the four developed categories to arrive at a measure of the fraction of each cell's land area that is developed (i.e., covered in constructed materials). We observe this variable in 1996 and 2010, the earliest and latest years for which we have complete Landsat data.[15]

2.3. SLR data

Our data on sea level rise come from detailed maps of areas anticipated to be inundated for various future sea level rise scenarios, which we obtained from NOAA's digital coast platform (Marcy et al., 2011).[16] The maps we use show inland extent of inundation for scenarios of sea level rise from 0 to 6 ft. Importantly, the mapping process also takes account of major federal leveed areas, which are assumed, for the purposes of creating these inundation maps, to be high enough and strong enough to prevent inundation, regardless of the SLR scenario (e.g., the SLR maps assume that New Orleans is safe even from 6-foot of SLR.).

In our analysis we focus on the share of an area (e.g., a block), which would be under water at high tide if SLR is 1 foot (approx. 30.5 cm). Information on sea level rise was added to the blocks (and cells) by intersecting the shapefiles for blocks (cells) with shapefiles of areas expected to be inundated for 1ft of sea level rise using GIS software. We then calculate the share of each census block (or cell) that is exposed to 1ft of sea level rise, which we refer to as $SLR1ft$. We further define low-risk areas as blocks (or cells) in our data where $SLR1ft = 0$; medium-risk, where $SLR1ft \in (0, 0.5]$; and high-risk, where $SLR1ft \in (0.5, 1]$. Of the blocks in our sample, 86% are low risk. Overall, the mean share of 1ft SLR for the entire sample of blocks is 0.046, and the area-weighted mean share is around 0.19.

2.4. Building restrictions data

Our dataset also includes information on areas where building construction may be restricted. While such restrictions may be an endogenous response by governments at different levels to the danger of building close to the coast, we nevertheless examine the role that such regulations may have in our setting. In the Data Appendix we discuss three different types of regulations: restricted areas, where housing development may be particularly constrained, and other zoning data; state "setback lines" close to the coast, beyond which construction may be more regulated; and local government regulations on building density.

2.5. Government subsidies and additional data

Data on historical damages from coastal flooding are taken from the National Flood Insurance Program (NFIP), operated by FEMA, which subsidizes flood insurance provision. In particular, we use data on insured losses from coastal floods, available at the census tract level, from 1973 to 2019. There are two points to note about NFIP. First, NFIP includes an implicit subsidy component.[17] For example, the Congressional Budget Office (CBO, 2017) notes that in 2016, "the overall shortfall of \$1.4 billion is attributable largely to premiums' falling short of expected costs in coastal counties, which constitute roughly 10 percent of all counties with NFIP policies but account for three-quarters of all NFIP policies nationwide … the net short- fall measured over all coastal counties is \$1.5 billion, whereas the net surplus measured over all inland counties is \$200 million." A recent analysis concluded that while NFIP's shortfalls cannot be attributed to any single incident, it borrowed significantly following Hurricanes Katrina in 2005 and Sandy in 2012. In 2017, as NFIP reached its borrowing cap of \$30.5 billion, Congress canceled \$16 billion of its liabilities, to allow NFIP to borrow more in response to Hurricanes Harvey, Irma, and Maria (Peter G. Peterson Foundation, 2020). It is also noteworthy that by our estimates, claims made to NFIP grew at a rate of around 4–5 percent in real terms from 1978–2019. While claims made under the NFIP do not reflect the totality of economic losses from coastal floods (or in fact the totality of residential losses from flooding, as some damage is uninsured), the NFIP data have the advantage of being available at a relatively fine level of geographic disaggregation – the census tract level – which makes these data well suited to our task of estimating how damages from flooding vary with distance from the coast. We convert these claims data – and all cost data – to 2020 US

[11] What we refer to as "2010" is more precisely data for 2006–2010 from the American Community Survey.

[12] Just over a fifth (22.4%) of blocks in our sample were empty – i.e., had zero housing units – in 1990.

[13] These categories include various classifications of open water, wetlands, agricultural land, forest etc., as detailed here: https://coast.noaa.gov/digitalcoast/training/ccap-land-cover-classifications.html.

[14] The four developed categories in the Landsat data are: "developed - high intensity" where constructed materials account for 80 to 100 percent of the total cover at that location; "developed medium intensity" (50–79 percent constructed material); "developed - low intensity" (21–49 percent); and "developed - open space", where constructed material accounts for less than 20 percent of land cover.

[15] Our cells dataset includes over 6 million observations, or cells within 10 km of the Atlantic and Gulf coasts. The mean share developed in 1996 is 0.066. More than 70% of cells in our data have share developed = 0 in 1996. By construction, the share developed measure is top coded at 0.9, but there are fewer than 7,000 cells in our data with this value for developed share in 1996.

[16] While these maps reflect the state of understanding about SLR towards the end of our study period, is consistent with our goal of explaining construction in recent decades on SLR-prone area assuming that people are individually rational and forward looking. Imperfect knowledge and understanding may further exacerbate the costs of SLR in the real world.

[17] In 2012 the Biggert-Waters Flood Insurance Reform Act was introduced in an attempt to phase out subsidies on the NFIP and bring the program towards fiscal solvency. These reforms proved controversial, particularly with respect to the impact on homeowners facing large increases in flood risk premiums. The 2014 Homeowners Flood Insurance Affordability Act partially repealed and modified the Reform Act (Bakkensen and Barrage, 2021).

Table 1
(Stylized fact 1) Much construction near the coast took place in areas with SLR risk.

	(1) Housing units in risky blocks (millions)	(2) Housing units in all blocks (millions)	(3) Fraction of housing units in risky blocks (%)
1990	1.77	14.87	12%
2010	2.62	18.11	14%
Change (1990–2010)	0.85	3.24	26%

Notes: Column (1) reports numbers of housing units in census blocks whose centroids are within 10 km of the coast and where at least some portion of the census block will be under water at high tide if sea levels rise by 1 foot (30.4 cm). Column (2) reports numbers of housing units in all blocks whose centroids are within 10 km of the coast. Column (3) reports the fraction of housing units in census blocks whose centroids are within 10 km of the coast that are also in blocks where at least some portion of the census block will be under water at high tide if sea levels rise by 1 foot (30.4 cm).

dollars using a GDP price deflator (Federal Reserve Bank of St. Louis, 2020). We then aggregate the damages data across the entire period available (1973–2019). To obtain a measure of damage per housing unit, we divide the total damages by the number of housing units in each tract from 2014–2018 (Manson et al., 2019).

Information on public spending associated with coastal flooding, which we use to calculate the share of damages subsidized by the taxpayer, was largely sourced from a recent Congressional Budget Office report (CBO, 2019). This report estimates that \$19.4 billion of taxpayer money is spent annually on mitigation of and relief from the damages caused by hurricanes.

Government subsidies to flood-prone areas also come in the form of constructing and maintaining flood defenses. The SLR data we use account for existing flood defenses (major federal leveed areas) and assume that these remain protected under any SLR scenario. Initiatives to build major new flood defenses raise concerns about costs to taxpayers, time to build, effectiveness as sea levels rise, and potential environmental damage (See for example a discussion of possible flood defense schemes for New York City: https://www.nytimes.com/2020/01/17/nyregion/the-119-billion-sea-wall-that-could-defend-new-york-or-not.html). Additional data sources used for our model simulation are detailed in Appendix Table A8, and we discuss the parameter estimates themselves in Section 4.5.1.

3. Empirical findings

This section documents two novel stylized facts about changes over time in coastal housing risk, and four auxiliary findings about the cross-section of coastal housing; we focus on the area which lies within 10 km of the US Atlantic and Gulf coasts, as discussed in Section 2. First, we present the two stylized facts, which are the focus of our study. Second, to set these in context, we describe three auxiliary findings on the location of coastal housing in the cross-section. Third, we show one additional finding, pertaining to the mechanisms that underlie coastal housing construction. Finally, we return to the two stylized facts and discuss their robustness.

3.1. Two stylized facts on changes in the risk of coastal housing

The first stylized fact is that **while historic construction near the coast avoided SLR-prone locations, more recent construction has not**. This is shown in Table 1. In 1990, areas with medium or high SLR risk accounted for about 12% of the housing units in our area of study. But from 1990–2010, 26% of net new construction took place in medium or high-risk blocks. Consequently, the fraction of the 2010 housing stock on SLR-prone locations was 14%.

The second stylized fact tells us where the risky new developments took place: **Recent construction in SLR-prone areas took place in dense locations, but not in sparse ones**. Table 2 reports regression estimates using the specification:

$$\Delta hunits_i = \beta_{11} + \beta_{12} SLR1ft_i + \epsilon_{1i}, \tag{1}$$

Table 2
(Stylized fact 2) SLR-prone areas were developed in dense tracts but not in sparse ones.

Housing units per sq km (1990)	(1) ≤10	(2) (10, 100]	(3) (100, 1000]	(4) >1000
Share 1ft SLR	−3.16***	−3.18***	2.26***	6.76***
	(1.07)	(0.82)	(0.80)	(2.03)
Constant	4.16***	7.59***	5.72***	4.62***
	(0.32)	(0.20)	(0.12)	(0.17)
Observations	24,927	149,461	283,208	86,471

Notes: The outcome in each case is the change in housing units at the block level from 1990–2010. Columns divide the data by levels of housing units per square km in census tracts (1990), excluding own block. Standard errors in parentheses are clustered by CBSA, with non-CBSA blocks grouped into a single cluster. For reference, urban population density is defined as at least 386 people (not housing units) per square km. Results robust to controlling for log distance to the coast. Significance: $^{*}p < 0.1$; $^{**}p < 0.05$; $^{***}p < 0.01$.

where $\Delta hunits_i$ is the change in the number of housing units in census block i, $SLR1ft_i$ is the share of the area of each census block, which will be under water at high tide if sea level rise (SLR) were 1 foot, or 0.305 m, and ϵ_{1i} is an error term, which is clustered by Core-based statistical area (CBSA) here and in all the spatial regressions we report below.[18] In interpreting $SLR1ft$ we note that it matters not only for a future with higher sea levels, but also for the present: areas with high $SLR1ft$ are more prone to both frequent low intensity "nuisance flooding" and to flooding from impactful events, such as tropical storms (Dahl et al., 2017). Therefore, all else equal, living in areas with high $SLR1ft$ likely involves costs (a point which we revisit below), and can be viewed as a disamenity. The regressions in Table 2 are estimated separately for four groups of census blocks, grouped by the housing density of the census tracts that contain them, where this density excludes the own block's density. As the table shows, in sparse census tracts, the growth in housing units is negatively associated with SLR. But in dense census tracts, new construction is positively associated with SLR proneness. All this suggests that where there is plenty of space to build, SLR-prone locations are avoided, in line with the evidence discussed above; SLR-prone locations are, however, built on in dense areas, presumably because no other local alternatives exist.

We highlight these two stylized facts because of their importance for understanding the growing risk from SLR and flooding in coastal areas from 1990–2010. Should these trends in coastal construction continue, the costs of flooding will rise rapidly in the coming decades.

[18] CBSAs include metropolitan statistical areas and micropolitan areas, and we add one cluster for all non-CBSA observations in the sample. In earlier versions of the paper, we obtained similar standard error estimates when clustering by state, an approach used by Donaldson and Hornbeck (2016) and others. We also explored using spatial clustering following Bester et al. (2011), using 1 × 1-degree clusters. This gave slightly smaller standard errors than those we report. Using Conley (1999) standard errors is more technically challenging in our setting, due to the large number of observations.

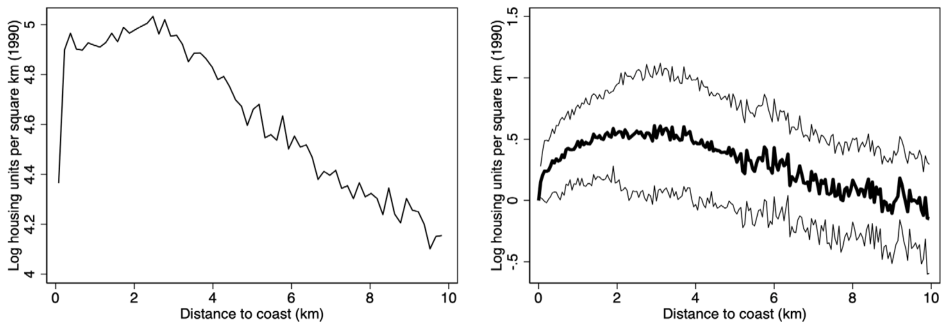

(a) (b)

Fig. 1. (Auxiliary Finding 1) Housing units concentrate near – but not right at – the coast. Panel (a) shows ln(housing units in 1990 per square kilometer) by distance to the coast for 150 m bins. The figure in Panel (a) is based on our full sample of blocks whose centroids are within 10 km of the US Gulf and Atlantic coasts. However, given that we partition the 10 km from the coast into 150 m bins, and take integers, the last observation, which is truncated (from 9.9–10 km from the coast) is excluded from the figure. The figure in Panel (a) therefore uses information from 542,246 census blocks. In Panel (a) housing units are taken from census data at the block level, while land area in each distance bin from the coast is taken from the Landsat gridded data. The gridded data are used for calculating area because for sparsely populated blocks or empty blocks, which often cover a large area, the centroid is inadequate for capturing their distance distribution from the coast, as described in more detail in the Data Appendix. Panel (b) shows regression coefficients and 95% confidence intervals from a regression of ln(housing units in 1990 per square kilometer) on 50 m distance bins. Standard errors in parentheses are clustered by CBSA, with non-CBSA blocks grouped into a single cluster. Housing units per square km in Panel (b) is calculated using housing units and land area from census data at the block level. The issue in relation to calculating land area noted above is less relevant here, since the regression restricts the sample to blocks with non-zero housing units (422,311 blocks).

To put these stylized facts into context, however, it is useful to look back at construction in coastal areas looked in 1990. With that objective in mind, we now proceed to characterize four auxiliary findings on the cross-section of coastal housing development.

3.2. *Auxiliary findings on the cross-section of coastal housing*

The first auxiliary finding we document is that **housing unit density peaks near – but not right at – the coast**. To show this, we calculate the number of housing units in each 150-meter distance bin from the coast, assigning the housing units in each census block to the bin where its centroid falls. We then normalize the total number of housing units in each bin by the area of that bin, which we approximate using the cells.[19] The results, in Panel (a) of Fig. 1, show that the logarithm of housing unit density peaks around 2.475 km from the coast, and declines asymmetrically, falling more rapidly on the coast side.[20] Specifically, housing density plummets close to the coast and declines more slowly on the inland side. A similar pattern can be seen in Panel (b) of Fig. 1, which restricts the analysis to census blocks with housing units, and reports point estimates and 95 percent confidence intervals from estimating the regression:

$$\ln\left(hdensity_i\right) = \beta_{21} + \beta_{22}\mathbf{Bin}_i + \epsilon_{2i}, \tag{2}$$

where $hdensity_i$ is the number of housing units per square km in census block i, $\mathbf{Bin}_i$ is a vector of indicators for 50-meter distance bins from the coast, and ϵ_{12} is an error term. The figure peaks around 3 km from the coast, and declines on both sides of the peak, again with a steeper decline on the coast side. As we discuss below, the steep decline near the coast side of Panel (b) understates the sparseness of housing density near the coast, since there are more empty blocks in the immediate vicinity of the coast; for that reason, we prefer the specification in Panel (a). We repeat the analysis of the two panels above in Panels (a) and (b) of Appendix Figure A2, this time excluding restricted areas (as discussed in the Data Section).[21] The results are largely unchanged.[22] Panel (c) of Figure A2 repeats the analysis of panel (a) of Fig. 1 but using only block-level data, for area as well as housing units. Here we use 50-meter bins, and the decline in density near the coast is even steeper. Finally, Panel (d) of Appendix Figure A2 repeats the analysis of panel (a) of Fig. 1 using cell-level data on built area instead of housing units. Using the built area data allows us to examine the extent not only of residential housing, but also of commercial and industrial areas, as well as roads and other artificial structures. Here the distribution peaks around 2 km from the coast, and once again the decline on either side is asymmetric and similar in magnitude to that in Fig. 1.

In interpreting the above-mentioned housing distribution, it is worth noting several additional empirical regularities. Commuting remains an important aspect of cities, and the vast majority of housing units that we consider are primary residences, where people live throughout most of the year. Specifically, only around 1 percent of the housing units in our sample are second homes.[23] Since we do not have fine-grained data on business activity, we assume in the discussion below that peak housing density corresponds to the location of the Central Business District (CBD). We note that given the limitations of our data we cannot explore multiple employment centers within the city, although we discuss this possibility below.[24]

[19] Census block centroids provide a good approximation of housing location, since areas with dense housing are partitioned into small blocks. But block centroids are less precise when it comes to measuring area, because areas with sparse housing (or no housing) tend to be in large census blocks. Using cell data to approximate land area in each distance bin is therefore more reliable, since the cells are by construction evenly distributed, and of equal size.

[20] The housing density is similar in its peak and in nearby distance bins, and it displays some geographic variation. For example, in the US South, housing density peaks closer to the coast, consistent with a higher amenity value of the beach. But in each subsample that we examined, density falls steeply very close to the coast and more gradually further away from it.

[21] As discussed in Section 2, we have no data on the location of all setback areas where construction is more regulated. Their existence may contribute to the steep fall in housing density within around 150 m from the coast but is unlikely to drive the overall pattern where housing density peaks around 2–3 km from the coast.

[22] Similarly, controlling for the Density Restriction Index (DRI) has little impact on the patterns shown in Panel (b) of Fig. 1 (results available on request).

[23] While the share of second homes rises in the immediate vicinity of the coast, it is still less than 7 percent even there. We also note that mobile homes make up only around 5 percent of our sample.

[24] The equivalent figures to Panels (a) and (b) for 2010 reveal a very similar picture; the peak of the housing density moves 300 m inland in the 2010 equivalent of Panel (a) but stays constant in the equivalent of Panel (b). In Section 4.5.2 we consider cases where the CBD moves over time.

Table 3
Places near the coast are asymmetric, with CBD closer to the coast.

	(1) Asymmetry
Distance to coast bins (km) ∈ [0, 1)	0.14***
	(0.03)
Distance to coast bins (km) ∈ [1, 2)	0.14***
	(0.03)
Distance to coast bins (km) ∈ [2, 3)	0.08***
	(0.02)
Distance to coast bins (km) ∈ [3, 4)	0.07**
	(0.03)
Distance to coast bins (km) ∈ [4, 5)	−0.01
	(0.03)
Distance to coast bins (km) ∈ [5, 6)	−0.00
	(0.04)
Distance to coast bins (km) ∈ [6, 7)	−0.04
	(0.03)
Distance to coast bins (km) ∈ [7, 8)	−0.02
	(0.03)
Distance to coast bins (km) ∈ [8, 9)	−0.05
	(0.03)
Constant	0.54***
	(0.03)
Observations	1,583

Notes: (Auxiliary finding 2) Census-designated places near the coast are asymmetric, with CBD closer to the coast. This table reports results from a regression of place asymmetry on 1 km distance bins from the coast. Standard errors in parentheses are clustered by CBSA, with non-CBSA places grouped into a single cluster. Place asymmetry is defined as the ratio of the distance $|X_R - X_0|$ to the distance $|X_R - X_L|$. The sample here is restricted to places for which the mean distance to coast from the centroids of blocks within that place is less than 10 km. The omitted category is [9, 10) km from the coast. Significance: $^{*}p < 0.1$; $^{**}p < 0.05$; $^{***}p < 0.01$.

Our second auxiliary finding is related to the first, namely that **census-designated places close to the coast are asymmetric**. To show this, we use data on places and their CBDs to estimate regressions of the form:

$$asymmetry_j = \beta_{31} + \beta_{32}\mathbf{Bin}_j + \epsilon_{3j}. \tag{3}$$

Here $asymmetry_j$ is the ratio $\frac{|x_R - x_0|}{|x_R - x_L|}$, where the numerator is the distance from each place's furthest point from the coast to its CBD, and the denominator is the distance from each place's furthest point from the coast to its nearest point to the coast; $\mathbf{Bin}_j$ is a vector of indicators for 1 km distance bins from the coast; and ϵ_{3j} is an error term.[25] As Table 3 shows, places whose centroids are within 4 km from the coast are asymmetric: the distance from their CBD to their inland edge is roughly double the distance from their CBD to the coast side edge. In contrast, places around 4–10 km from the coast are roughly symmetric. An example of this can be seen in Appendix Figure A3, which shows places in the Greater Boston area: those close to the coast are asymmetric, while those further away are more symmetric.

The third auxiliary finding is that **the asymmetry near the coast is more pronounced for large places**. We show this by using the place-level data to estimate regressions of the form:

$$asymmetry_j = \beta_{41} + \beta_{42}size_j + \beta_{43}\ln\left(dist\_coast_j\right) + \beta_{44}\left[size_j \cdot \ln\left(dist\_coast_j\right)\right] + \epsilon_{4j}, \tag{4}$$

where $size_j$ measures the size of place j, either as $\ln\left(area_j\right)$ where the area is in square kilometers or as the distance $\left|x_R - x_L\right|$ in km; $\mathbf{dist\_coast}_j$ is the mean distance from each place's blocks to the coast; and ϵ_{4i} is an error term. The estimates in columns (1) and (2) of Table 4, which add the restriction $\beta_{43} = \beta_{44} = 0$, show that on average, larger places (using either of the above measures) are more asymmetric. Columns (3) and (4), which are unrestricted, show that the asymmetry is more pronounced for large places when their CBDs are closer to the coast.

3.3. Auxiliary findings on mechanisms that shape the coastal housing distribution

Whereas the three auxiliary findings above tell us how economic activity concentrates near but not right at the coast, here we present evidence about why this is the case. Our fourth auxiliary finding is that **blocks prone to SLR are much more sparsely built on, and among the SLR-prone blocks, those further from the coast are even more sparsely built.** To examine how much SLR-prone blocks are avoided, we split the census blocks into three groups: high-risk, medium-risk, and low-risk, as discussed in Section 2. We then repeat the analysis in Panel (a) of Fig. 1 separately for each of the three groups of blocks. The results in Fig. 2 show that at every distance bin from the coast, low-risk census blocks are about two to three times more densely built than medium-risk blocks, while the medium-risk ones are, at most distance bins, several times denser than the high-risk ones. These results are confirmed in robustness checks that we report in Figure A4, where we repeat the analysis in Fig. 2 excluding the restricted areas (Panel (a)) and then using the fraction of cell area that is built, based on our gridded data (Panel (b)). When we look within each risk group, especially the for the two riskier groups, housing density tends to increase as we approach the coast. In other words, people seem to understand SLR risk and avoid it, even as they value proximity to the coast. This is consistent with the observation that as we approach the coast, SLR-proneness rises steeply. As Panel (a) of Fig. 3 shows, the proportion of low-risk blocks is consistently over 90% in the 3–10 km area from the coast. However, as we get closer to the coast within the three km range, this proportion declines rapidly to less than 20%, while the proportion of medium-risk and high-risk blocks increases significantly. Panel (b) of Fig. 3 reports the mean $SLR1ft$ by distance to the coast. This share is lower than 5% in the area 1–10 km from the coast but increases steeply to almost 45% as we get very close to the coast. Appendix Figure A5 shows that these results are again robust to excluding restricted areas. Together, this evidence suggests that the amenity of proximity to the coast, which increases gradually, is offset by a convex disamenity due to flood risk as we near the coast.

To see why this matters, we demonstrate the steep rise in damages from flooding as approach the coastal areas in Fig. 4, which shows the point estimates and 95% confidence intervals from the regression:

$$\ln\left(damage_k\right) = \beta_{51} + \beta_{52}\mathbf{Bin}_k + \epsilon_{5k}, \tag{5}$$

where $damage_k$ is the total dollar sum of NFIP claims from 1973–2019 (in 2020 USD), normalized by an estimate of the number of housing units from 2014–2018 in census tract k; $\mathbf{Bin}_k$ is a vector of indicators for 150-meter distance bins from the coast; and ϵ_{5k} is an error term.[26] As the figure shows, claims in the distance bin closest to the coast are about 2.5 to 3 log points (or about 12–20 times) higher than in the areas around 4–10 km from the coast. While NFIP claims represent only a fraction of the total costs of flooding over the past few decades, this figure indicates that flood costs rise convexly as we approach the coast.[27]

[25] Our asymmetry measure, $\frac{|X_R - X_0|}{|X_R - X_L|}$, is for the most part, bounded on the interval [0,1]. There is a small minority of cases where the measure exceeds 1, since in reality X_R, X_0, and X_L are not all on one line. Nevertheless, excluding these few cases does not substantively affect our estimates.

[26] The use of the recent housing units measure mitigates the risk that NFIP claims per housing unit will appear large near the coast because housing expanded there, as we discuss below. The patterns we document are, however, robust to using 1990 housing units in the denominator.

[27] As we discuss in the Data Appendix, NFIP costs cover only a fraction of total damages from flooding. The low uptake of NFIP flood insurance, as well as the presence of demand frictions and selection biases, may introduce

Table 4
Bigger places are more asymmetric, conditional on being near the coast.

	(1) Asymmetry	(2) Asymmetry	(3) Asymmetry	(4) Asymmetry
Ln($\lvert X_R - X_L \rvert$)	0.015*		0.332***	
	(0.008)		(0.053)	
Ln(area)		0.028***		0.178***
		(0.005)		(0.032)
Ln(Distance to coast)			0.114*	0.225***
			(0.067)	(0.069)
Ln($\lvert X_R - X_L \rvert$)*Ln(Distance to coast)			−0.030***	
			(0.008)	
Ln(area)*Ln(Distance to coast)				−0.018***
				(0.004)
Constant	0.497***	0.166**	−1.102**	−1.749***
	(0.067)	(0.081)	(0.451)	(0.525)
Observations	1,583	1,583	1,583	1,583

Notes: (Auxiliary finding 3) Bigger census-designated places are more asymmetric, conditional on being near the coast. This table reports results from regressions of place asymmetry on measures of place size, place distance to the coast, and their interaction, all in logs. Place asymmetry is defined as the ratio of the distance $\lvert X_R - X_0 \rvert$ to the distance $\lvert X_R - X_L \rvert$. The area variable is the sum of the area of blocks that are within a place's boundaries. The sample here is restricted to places for which the mean distance to coast from the centroids of blocks within that place is less than 10 km. Standard errors in parentheses are clustered by CBSA, with non-CBSA units grouped into a single cluster. Significance: *p < 0.1; **p < 0.05; ***p < 0.01.

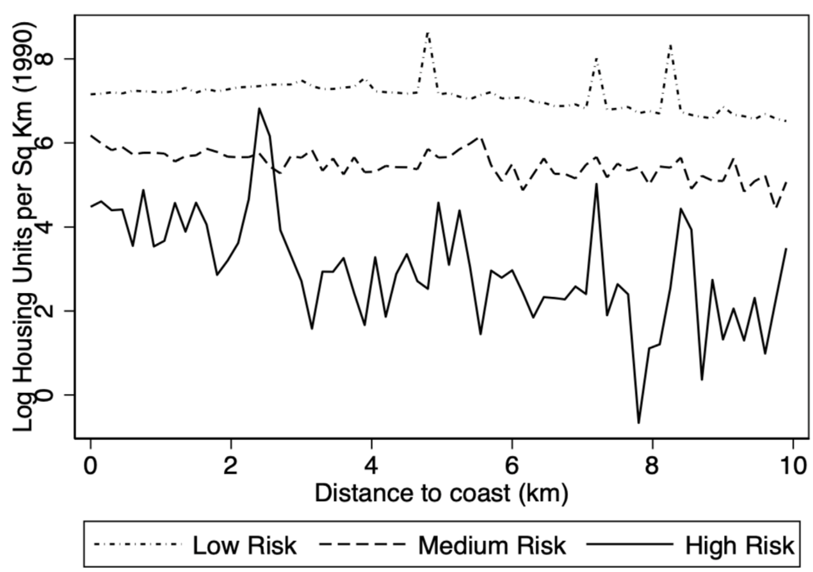

Fig. 2. (Auxiliary Finding 4) Areas that are highly prone to sea level rise (SLR) are less built. The figure shows the log of average block level density (housing units per square kilometer in 1990, based on census data) by distance to the coast in 150 m bins, and share of area under water with 1 foot of sea level rise. The three risk categories are defined by the share of each census block that will be under water at high tide if sea levels rise by 1 foot (30.4 cm): we label blocks as high risk if the share of 1ft SLR is > 0.5, as medium risk where 0 < share 1ft SLR <= 0.5, and as low risk where share of 1ft SLR = 0. This risk reflects odds of flooding even today, without any SLR. As the figure shows, at each distance from the coast, the riskier areas are more sparsely built.

Having characterized the four auxiliary findings, we now examine the distribution of prices near the coast. Panel (a) of Figure A6 reports estimates using the same specification as Panel (c) of Fig. 1, except plotting the fraction of blocks in each 50-meter distance bin from the coast, for which median house prices are missing. Median prices are missing if blocks are empty or very sparsely populated, so that disclosing moments from the price distribution would reveal information about individual housing units. The figure shows that median house prices are missing for about 30 percent of the census blocks from around 1–10 km from the coast. In the 1 km closest to the coast, however, the fraction missing rises steeply to almost 67 percent in the blocks closest to the coast. Panel (b) shows that where median house prices are available, they are also fairly flat around 1–10 km from the coast, rising steeply in the 1 km closest to the coast. Interpreting this pattern is not straightforward, because of the missing blocks; the coverage within blocks (only 64.1% of housing units in 1990 were owner-occupied); differences in housing characteristics within locations and across them; and the use of the median. Nevertheless, at first glance, the findings we document may seem surprising: blocks near the coast are flood-prone and much sparser than others, and this sparseness is not driven by restricted areas, as Panels (a) and (b) of Fig. 1 show; yet where house prices are recorded there, they are high. We explain this apparent puzzle below in the extensions, by noting that while locations in blocks close to the coast are generally flood-prone and therefore in low demand, there may be small higher-elevation areas within these

measurement discrepancies. Another concern is the SFHA designation, particularly for inland areas. Despite these limitations, we utilize NFIP data in this study because it provides spatially disaggregated information at the census tract level. Excluding restricted areas at this level of analysis is unnecessary due to the larger scale of census tracts, which primarily focus on built areas.

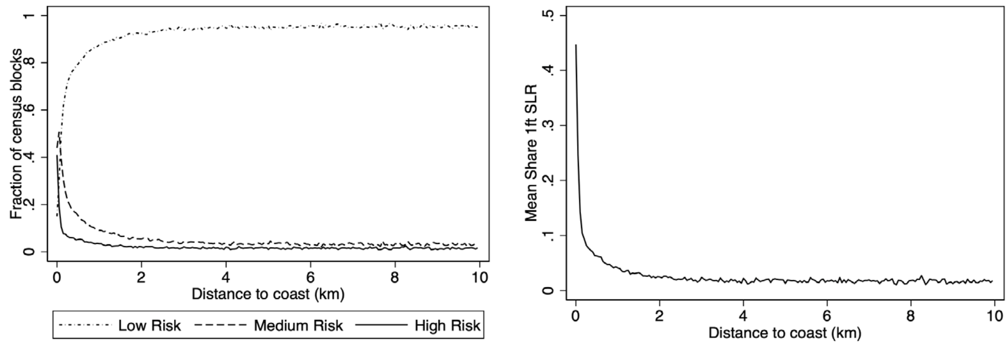

(a) (b)

Fig. 3. Flood risk helps explain why people do not build right on the coast. Panel (a) shows the fraction of census blocks in each risk category by distance to the coast in 50 m bins. The three risk categories are defined by the share of each census block that will be under water at high tide if sea levels rise by 1 foot (30.4 cm): we label blocks as high risk if the share of 1ft SLR is > 0.5, as medium risk where 0 < share 1ft SLR <= 0.5, and as low risk where share of 1ft SLR = 0. This risk reflects odds of flooding even today, without any SLR. Panel (b) shows the mean share of block area that is subject to 1ft SLR, by distance to the coast in 50 m bins.

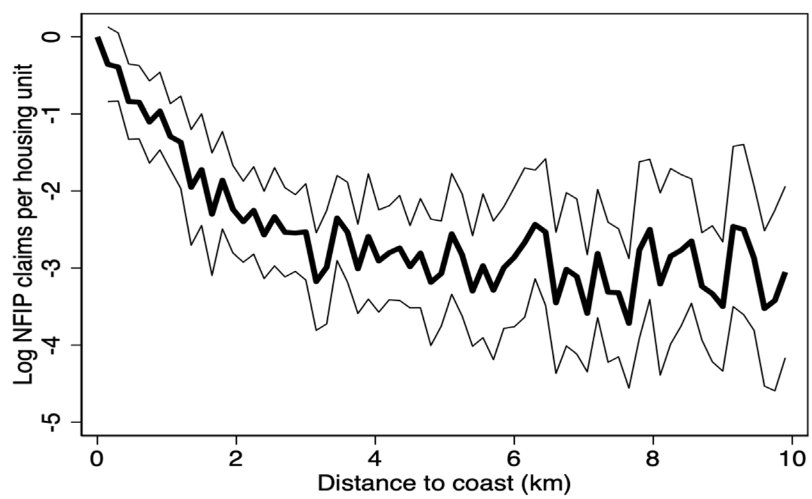

Fig. 4. Damages from flooding decline rapidly with distance from the coast. The figure shows the estimated coefficients and 95% confidence interval from a regressions of log NFIP claims per housing unit, on 150 m distance bins from the coast. Standard errors in parentheses are clustered by CBSA, with non-CBSA units grouped into a single cluster. The NFIP claims data are for the years 1973–2019, observed at the census tract level, and have been converted to 2020 US dollars. Housing units are also observed at the census tract level, and are taken from 2014–2018 estimates. Full details of the data sources used are included in the Data Appendix.

blocks, where flooding is much less of a problem, and where prices are high.

Returning to our first four auxiliary findings, we note that Auxiliary Finding 4 helps explain Auxiliary Findings 1-3: conditional on risk, people seem to prefer to live as close as possible to the coast, but as we approach the coast risks increase steeply. This gives rise to the distribution of housing density, which peaks near the coast and declines asymmetrically, falling more steeply on the coast side than on the inland side.

3.4. Robustness of the stylized facts on changes in coastal housing risk

Whereas the four auxiliary findings describe coastal area housing at a point in time, mostly around 1990, our two (main) stylized facts describe how they changed from 1990–2010. Appendix Table A1 reports regression estimates from specification (1) for the full sample, using as outcomes 1990 housing units and the change in housing units from 1990–2010. Columns (1) and (2) of Panel A show that 1990 housing units are strongly negatively correlated with $SLR1ft$, but for 1990–2010 this correlation is close to zero. Subsequent columns show that these relationships are robust to controlling for CBSA fixed effects and restricting the sample to only urban (CBSA-located) blocks, and Panel B shows estimates controlling for distance bins to the coast, as well as (again) CBSA fixed effects. The final columns of Panel B, with a full set of controls show a strongly negative correlation of construction and SLR risk in 1990, and a positive though imprecise relationship for changes from 1990–2010.

Next, we revisit the baseline estimates of Stylized Fact 2 as reported in Table 2. We now add CBSA fixed effects and distance bins to the coast, and restrict the sample to CBSAs, and report combinations thereof. Appendix Table A2 shows that the results are robust: in sparse census tracts, areas prone to SLR were avoided from 1990–2010, while the opposite was true in dense census tracts. In Appendix Table A3 we return to the specifications estimated in Table 2, but this time excluding restricted areas, and the pattern is again robust. Finally, in Appendix Table A4 we repeat the analysis using the cell data on built area, where this time "neighborhoods" are larger (1 square km) areas, whose fraction built we calculate excluding the own cell. In sparse "neighborhoods" new construction was strongly negatively correlated with SLR risk, while in the densest "neighborhoods" the correlation is positive though imprecisely estimated. This imprecision may arise because it is harder to detect the densest locations using the satellite imagery data, which only measure whether each pixel is built and not how densely it is built.

To further investigate the role of amenity in shaping Stylized Fact 2, we use winter weather as a demand shifter (Rappaport, 2007) and examine whether in areas that grew faster due to good weather there was a difference in construction on SLR-prone locations between dense and sparse census tracts. Specifically, we estimate regressions of the type:

$$\Delta hunits_i = \beta_{61} + \beta_{62} SLR1ft_i + \beta_{63} Mildwinter_i + \beta_{64} Mildwinter_i * SLR1ft_i + \epsilon_{6i}, \quad (6)$$

where $Mildwinter_i$ measures higher January temperatures or an index of mild winters more generally (see details in Appendix Table A5) and ϵ_{6i} is an error term. Columns (1) and (2) of Appendix Table A5 confirm that locations with mild winters experienced faster growth in the number of housing units from 1990–2010, consistent with Rappaport (2007). More importantly, the rest of the table shows that this growth was uneven: in sparse census tracts, the interaction of mild weather and $SLR1ft$ is weakly negative, while in dense census tracts it is strongly positive. This suggests that growing demand for housing translates into risky construction locations only where housing is already densely built, and few alternatives remain. To illustrate the construction locations in dense, SLR-prone areas from 1990–2010, Appendix Figure A7 shows four case studies of developments in the fringes of dense tracts: Revere and Chelsea in Greater Boston, Massachusetts; Jamaica Bay and Rockaway Peninsula in the borough of Queens, New York City, New York; Miami Beach and Miami, Florida; and Clearwater and Largo, Tampa Bay area, Florida. Construction in the two areas in Florida is particularly pronounced, as we can expect from the findings in Appendix Table A2.

Finally, we show in an extension to Stylized Fact 2 that **in the densest census tracts, new construction focused on medium risk rather than high-risk areas**. To show this, Table 5 reports estimates from two regressions, which restrict the analysis to the densest group of census tracts discussed above. Column (1) uses specification ((2)), but with the change in housing units in each census block from 1990–2010 as the dependent variable and an exhaustive set of bins for different percent SLR in each census block.[28] Column (2) is the same, except that the regressors are an indicator $I_{SLR1ft>0}$ (that is, medium or high risk) and a continuous measure ($SLR1ft$). Both specifications tell a similar story: new construction took place in medium-risk areas more than in low-risk areas, but the highest risk areas were still generally avoided. Appendix Table A6 shows that these results are robust to excluding restricted areas. Finally, Appendix Table A7 repeats the analysis, this time using the cells instead of blocks (as discussed above), and the results are again similar to those in Table 5.

Table 5
(Extension of fact 2) SLR-prone areas developed in dense tracts were those with least SLR.

	(1)	(2)
Share 1ft SLR ∈ (0.0, 0.1)	13.53	
	(8.66)	
Share 1ft SLR ∈ [0.1, 0.2)	15.91***	
	(4.76)	
Share 1ft SLR ∈ [0.2, 0.3)	8.26***	
	(2.49)	
Share 1ft SLR ∈ [0.3, 0.4)	16.53**	
	(6.92)	
Share 1ft SLR ∈ [0.4, 0.5)	10.40	
	(8.59)	
Share 1ft SLR ∈ [0.5, 0.6)	4.54	
	(4.18)	
Share 1ft SLR ∈ [0.6, 0.7)	−0.33	
	(3.66)	
Share 1ft SLR ∈ [0.7, 0.8)	−2.60	
	(4.18)	
Share 1ft SLR ∈ [0.8, 0.9)	−2.85	
	(1.97)	
Share 1ft SLR ∈ [0.9, 1.0)	−2.79	
	(2.10)	
Share 1ft SLR ∈ 1	−3.88***	
	(1.21)	
Some SLR		15.83**
		(6.65)
Share 1ft SLR		−19.40*
		(9.93)
Constant	4.24***	4.24***
	(1.41)	(1.41)
Observations	86,471	86,471

Notes: This table reports coefficients from two regressions where the outcome is the change in housing units at the block level from 1990–2010. The sample here is restricted to blocks where tract housing density, excluding the own block, exceeds 1000 housing units per square km. The omitted category, 0 SLR, accounts for 95.5% of the blocks with this level of tract housing density in 1990. Standard errors in parentheses are clustered by CBSA, with non-CBSA units grouped into a single cluster. In column (2), the variable $SomeSLR$ is an indicator for blocks that have share 1ft SLR >0, while $Share1ftSLR$ is a continuous measure of the share of each block prone to 1ft SLR. Results robust to controlling for log distance to the coast. Significance: *p < 0.1; **p < 0.05; ***p < 0.01.

4. Model

In this section, we introduce a model of coastal development that reconciles the stylized facts and auxiliary findings discussed earlier. The model is parsimonious and designed primarily to build intuition, provide qualitative insights, and explore counterfactual scenarios. We begin this section by outlining the model's assumptions. We then characterize the equilibrium and relate it to our empirical findings. Finally, we extend the model to consider several counterfactual scenarios, and cautiously explore potential welfare implications.

4.1. Baseline assumptions

The model is in discrete time, and periods are denoted by t. Spatially, we extend the monocentric city model (Alonso, 1964; Mills, 1967; Muth, 1969), by placing it in the context of a coast, proximity to which offers both benefits and costs. The key geographic locations of the city are the CBD, denoted by x_0; the coast-side and inland edges of the city, denoted by x_{Lt} and x_{Rt}; and the coast itself, whose initial location is normalized to 0.[29] Initially, the CBD location is chosen by a historical city founder, and then the city persists for T periods (decades). In each period, developers choose where to build, taking into account the preferences of residents, who choose where to locate.

The city founder is assumed to be myopic, and chooses a location x to maximize their locational utility

$$U^F(x) = -\theta_1 x - \theta_2 x^{-\sigma}. \quad (7)$$

As we discuss below, to rationalize our empirical findings, we assume that $\theta_1 > 0$, reflecting our observation that proximity to the coast has an amenity value (air, views, bathing), which we assume is linear.[30] For the same reason, we also assume $\theta_2 > 0$ and $\sigma > 0$, reflecting a convex disamenity (higher risk of flooding).[31] As discussed later, the

[28] In line with Stylized Fact 1, we note that in dense locations, blocks with low shares of SLR saw larger increases in housing unit growth than those with no SLR (captured by the omitted category).

[29] Later, when we explore SLR, we relax this assumption by allowing the initial location of the coast to shift inland over time.

[30] It is possible that across wider areas than the coastal band that we study, the amenity component of the utility function also declines convexly in distance to the coast. But the key assumption is that it is less convex than the disamenity term, so for simplicity we assume a linear amenity term in the vicinity of the coast, which is the area we focus on. As we discuss below, this assumption is motivated by the convex increase in flood risk as we near the coast.

[31] To keep the model simple and allow for future extensions, we omit risk aversion, although our specification can be seen as a reduced-form way of capturing risk aversion. Moreover, the disamenity included in our model

pattern of housing density increasing and then decreasing as we move inland from the coast aligns with a demand-based explanation. We note that for simplicity, the model is deterministic, and the risk of flooding is captured by the last term of the utility function. We assume that the founder's chosen location becomes the city's CBD, x_0.[32]

There is a continuum $[0,\overline{x}]$ of competitive and forward-looking developers, each of whom owns a plot of land of measure 1 in location x; we assume that $\overline{x} > 0$ is sufficiently high not to constrain the land side development. Each period, each developer can allocate their plot to housing, which yields a period price of $p_t(x)$, or to agriculture, which has a period price p_A.[33] The developers' time preference is captured by $\delta \in (0,1)$, and in each period every developer maximizes their present-discounted stream of future prices.

Finally, we assume that there is a continuum of perfectly mobile residents with sufficient mass to populate the city. In every period $t = 1, \ldots, T$, each resident may live in the city or outside it. If a resident lives in the city, they inelastically supply one unit of labor, receive a wage, and spend their income on consumption and housing, in which case their utility is:

$$U(c_t(x), h_t(x), x) = c_t(x)^{\alpha} h_t(x)^{1-\alpha} - \theta_1 x - \theta_2 x^{-\sigma} \tag{8}$$

where $c_t(x)$ and $h_t(x)$ denote private consumption goods and housing in period t and location x, and $\alpha \in (0,1)$ is the consumption share of income. We assume that residents' preferences satisfy standard assumptions ($U_c > 0, U_h > 0, U_{cc} < 0, U_{hh} < 0$). The residents' locational preferences are the same as those of the city founder. The budget constraint of each resident in period t is:

$$p_t(x)h_t(x) + c_t(x) = w_t - |x - x_0| \tag{9}$$

where the price of consumption is normalized to 1; w_t is wage, and $|x - x_0|$ reflects the time cost of commuting. Each resident also has an outside option of living outside the city, with utility $\bar{U} > 0$. We initially consider a city whose attractiveness to residents and developers increases (at least weakly) relative to the outside option, or in other words that w_t increases (weakly) in t.

We solve the model as a Nash equilibrium, where developers take into account the expected maximization of other developers and of the residents.

4.2. Equilibrium

Here we summarize the equilibrium conditions of the model, a visual illustration of which is discussed in Section 4.5.2.

City founder: maximization of the city founder's decision implies, using the first-order condition, that

$$x_0 = \left(\frac{\sigma\theta_2}{\theta_1}\right)^{\frac{1}{\sigma+1}}. \tag{10}$$

We note that while our formulation of the model emphasizes a tradeoff between the risk and reward of locating near the coast, other historical factors relating to proximity to an agricultural hinterland and access to national and international markets may have also played a role in determining the historical locations of CBDs. Our analysis focuses on cities for which this balance meant that the CBD location is close to the coast.

Residents decide where to live and the share of consumption goods and housing in their consumption bundle. In equilibrium they are indifferent between all city locations, including the city endpoints, and their outside option $\bar{U}$. Residents' indifference between locations then determines the price function, $p_t(x)$, for each period.

Developers decide which locations should be part of the city, taking into account the present discounted stream of future prices. Since the baseline setup of the model is static, developers will build in all locations such that

$$p_t(x) \geq p_A. \tag{11}$$

Since (as we show below) prices decrease monotonically as we move away from the CBD, and the disamenity asymptotes near the coast, the boundaries of the city x_{Lt} and x_{Rt} are pinned down by the equations:

$$p_t(x_{Rt}) = p_t(x_{Lt}) = p_A. \tag{12}$$

Note that because of the assumptions discussed above, developers can repurpose land costlessly in every period, severing any dynamic link between periods. Below we discuss an extension where housing construction is costly and irreversible, which introduces dynamic considerations.

To complete the description of the equilibrium, we note that in each period, supply and demand for housing determine the price of land in each location, $p_t(x)$ and the city's population, $pop_t = \int_{x_{Lt}}^{x_{Rt}} \frac{1}{h_t(\hat{x})} d\hat{x}$.

4.3. Relating the model to the empirical findings

We now discuss how the model accounts for the two stylized facts and four auxiliary findings that we documented. We begin with Auxiliary finding 4, that flood-prone areas are more sparsely built, but holding flood risk constant proximity to the coast is seen as an amenity. This motivates our assumption that $\theta_1 > 0$. At the same time, Auxiliary findings 5 and 6 show that the cost of flooding rises convexly with proximity to the coast, motivating our assumptions that $\theta_2 > 0$ and $\sigma > 0$.

Next, we turn to Auxiliary finding 1, that housing density is single-peaked and decreases on both sides of the CBD.

Proposition 1. *Define housing density* $dens_t(x) \equiv \frac{1}{h_t(x)}$*, we get the following result:*

For each period $t = 1, \ldots, T$*: if* $x < x_0$ *then* $\dfrac{\partial \ln\left(dens_t(x)\right)}{\partial x} > 0$*;*

$$\text{if } x > x_0 \text{ then } \frac{\partial \ln\left(dens_t(x)\right)}{\partial x} < 0. \tag{13}$$

Proof. See appendix. ■

At this point we revisit the house price profile shown in Figure A6, which was quite flat from 1–10 km from the coast. This pattern is largely consistent with our model, as long as commuting costs account for a small share of income, which is what we find in Section 4.5.1 below. In the model, each resident spends a share $1-\alpha$ of their income on housing, and this corresponds to the price of their "housing unit". Proximity to the CBD grants individuals smaller, high-value land plots, while locations closer to the city's outskirts offer larger, more affordable land. And indeed, as our first auxiliary finding suggests, locations further from the CBD have fewer housing units per square km, or in other words more area per housing unit, consistent with the model. Nonetheless, we still need to address the issue of higher prices observed in sparsely populated areas within 0–1 km of the coast. We revisit this below where we consider a limited number of elevated coastal locations.

accounts for indirect effects of flooding on soil suitability for housing and the impact of wind gusts.

[32] The location of many cities on the US Atlantic and Gulf coasts was established more than a century ago, so for simplicity we assume that their location choices were myopic. We also ignore any productivity component in the city founder's locational choice, although adding this would not make much difference to the model overall.

[33] We follow the literature by labeling non-housing use as agriculture. In the baseline model we assume that agricultural prices are fixed across time and space, and that there is no cost of converting land across uses. We relax the latter assumption in an extension in Section 4.4.2. One caveat that we do not consider is salinity, which may affect some forms of agriculture, but not others (e.g., fishing).

Another characteristic of coastal areas, as highlighted in Auxiliary finding 2, is their asymmetry, with the CBD situated closer to the coast-side edge than the inland edge. We show that this is the case in the model.

Lemma 1. *The city develops asymmetrically around the CBD:* $|x_{Rt} - x_0| > |x_0 - x_{Lt}|$.

Proof. See appendix. ■

Our final static empirical result, Auxiliary finding 3, is that the asymmetry near the coast is more pronounced for large cities. And in the model, the city's asymmetry goes away if it is very small. This can be seen if we consider the minimal wage required to sustain the city, $\widetilde{w}$. As the wage falls to this minimum level and the city becomes very small, it is no longer asymmetric.

Lemma 2. *Vanishingly small cities are symmetric:* $\lim_{w_t \searrow \widetilde{w}} \frac{|x_{Rt}-x_0|}{|x_{Rt}-x_{Lt}|} = 0.5$.

Proof. See appendix. ■

Turning to the first of our stylized facts, we assume that the 1ft SLR area is closest to the coast, in a range $[0, D]$, where $D < x_0$. Historically, wages were low and cities we small, so the SLR-prone area is avoided. But as a cities grew, construction began to encroach on the SLR-prone area.

Lemma 3. *If w_t is sufficiently low, the city avoids SLR-prone areas ($x_{L0} > D$). But if w_t increases sufficiently, the city eventually expands into 1 ft SLR areas ($x_{L0} < D$).*

Proof. See appendix. ■

This result leads to a different perspective on the geographic constraints of the city than Saiz (2010) and Harari (2020), in whose work the city expands until it reaches "hard" edges. In contrast, our model allows for "soft" edges, which residents and developers would like to avoid, but which are developed regardless as the city expands.

Finally, we show that SLR-prone areas are developed in densely built locations, but not in sparse ones.

Lemma 4. *As long as the wage is low, the city is small and sparsely populated, SLR-prone locations are not developed; but as the wage increases sufficiently, population density rises, and SLR-prone locations are developed.*

Proof. Follows immediately from Lemma 3. ■

This provides an intuitive explanation to Stylized Fact 2, where expansion into flood-prone areas occurs in densely built locations.[34]

4.4. Extensions

Here we consider extensions of the baseline model including: sea level rise; irreversible housing construction; a limited number of elevated locations near the coast; government subsidies to partly offset the disamenity of proximity to the coast; multiple employment centers within the city; and land use regulations.

[34] This result does not prove that the share built on SLR-prone locations increases monotonically.

4.4.1. Sea level rise

We model sea level rise as a change in the location of the coast, x_{ct}. In this case, each resident's utility is

$$U(c_t(x), h_t(x), x) = c_t(x)^{\alpha} h_t(x)^{1-\alpha} - \theta_1 \left(x - x_{ct}\right) - \theta_2 \left(x - x_{ct}\right)^{-\sigma}. \quad (14)$$

For simplicity, we focus on the case where sea levels rise linearly, in a city which slopes linearly from the coast to the CBD, although the model can be adapted to nonlinear SLR. We assume that once a location becomes submerged due to sea level rise, it becomes uninhabitable. Sea level rise also affects the attractiveness of non-submerged areas. Locations on the coast-side of the CBD become less appealing because the costs of the disamenity rise at a faster rate than the benefits from the amenity, as observed in the city founder's problem. On the other hand, locations further inland may experience temporary benefits from sea level rise, as the amenity value of proximity to the coast outweighs the increased disamenity from flooding. Assuming a fixed CBD, this may lead to even greater asymmetry in coastal cities and result in higher average commuting costs. The issue of "misshapen cities" (Harari, 2020) may be further aggravated by SLR.[35]

4.4.2. Irreversible housing construction

The analysis thus far assumes a simplified scenario where developers can switch land use between agriculture and housing at no cost, making each period independent. To relax this assumption, we introduce a time cost associated with switching, creating a "dynamic" version of the model in contrast to the static baseline. To maintain tractability, we assume that converting land from agriculture to housing incurs a cost equal to one period's price and is irreversible (while conversion from housing to agriculture is infinitely costly). Developers solve their problem by comparing the present discounted value of prices across all time periods until T (or until the plot becomes submerged with sea level rise). So the developer's problem in city location x and period $t = 1, \ldots, T$ is:

$$\underset{t=1,\ldots,T}{Max} \left\{ \sum_{s=t}^{T} \delta^s p_A, \underset{\hat{s}=t,\ldots,T}{Max} \left[\sum_{t \le s < \hat{s}} \delta^s p_A + \sum_{T \ge s > \hat{s}} \delta^s p_s(x) \right] \right\}. \quad (15)$$

This condition replaces expression (12). The introduction of these costs dampens the incentives to expand the city, both due to the opportunity cost of receiving the agricultural price for a period (instead of developing) and because of the option value of developing later.

We note that the modeling assumption above relates only to extensive margin changes (whether land has housing or not), and not to intensive margin ones (how many units of housing it has). Adding frictions on the number of housing units is more analytically involved (see for example Henderson et al., 2020). We hypothesize that barriers to increasing housing density as the city expands contribute to the expansion of the extensive margin towards the coast and amplify the distortion caused by sea level rise.

4.4.3. Government subsidies

While the model we use is deterministic (for analytical simplicity), uncertainty plays a role in the lives of coastal dwellers. While in principle this leaves room for private insurance markets, in practice governments are usually heavily involved in providing flood insurance (including re-insurance), since the shocks that households suffer are not idiosyncratic, but correlated over large areas. In providing such insurance, governments often end up subsidizing coastal residents. This may happen, for example, because of outdated flood maps, which underestimate rising flood risks, as well as ex-post bailouts. Indeed, as we discuss in the data section, there is evidence that the US government subsidizes coastal development.

[35] Considering what happens to the city when its CBD is under water is beyond the scope of this paper.

Here we explore allocating government subsidy in proportion to the losses we document in Auxiliary finding 6 (in proportion to the fitted values from equation (19) below). This allows us to explore how subsidies affect city development, and how they interact with SLR.

4.4.4. Land use regulations

We consider two types of land use regulation: the first is aimed at reducing construction on flood-prone areas, while the second restricts land use within safer areas of the city (See for example Gyourko et al., 2019 for a discussion of local land regulations). To model regulations aimed at restricting construction in flood-prone areas, we consider them as a tax on housing, which decreases in the distance to the coast. The simplest case is a partial or full offset to any government subsidy (see above), which requires no further elaboration. Next, we consider the case of regulations that restrict housing supply in safer parts of the city. A typical policy is a green belt placed at the inland edge of the city. In an open city model where there are no migration frictions across cities, the attractiveness of building near the coast, will not be affected by the green belt. But in a closed-city version (e.g., Duranton and Puga, 2014), a green belt increases demand for housing in the sections of the city where construction is allowed, resulting in development further towards the coast. To illustrate this point, we revise our model by assuming exogenous population growth over time in a closed city model. Both wages and rents adjust to ensure that the equilibrium population, which is the aggregation of housing density over all developed land parcels, grows exogenously at a rate of 5% or 10% per period, similar to the growth rates in the open city model. The value of agricultural land is still pre-determined and identical to that of the baseline model.[36]

4.4.5. Additional extensions

In the appendix we consider two further extensions. One involves a finite number of elevated locations near the coast, which are safe and hence highly desirable; the other considers a case where employment is dispersed throughout the city, instead of being concentrated in a CBD.

4.5. Simulations

4.5.1. Parameter estimation

Below we study a synthetic low-elevation coastal city and explore its evolution under different assumptions and scenarios. Coastal cities vary, of course, in size and location, depending on local conditions and history. Our model therefore illustrates the conditions that may prevail in a city whose characteristics are similar to those we find when averaging across distances from the coast across the area we study. In the appendix we explain the choice of parameters we use to estimate the model under different scenarios. These parameters are reported in Appendix Table A8.

4.5.2. Simulation estimates

We summarize some aspects of the simulated model for 1990 in Appendix Figure A9. This figure shows the linear decline in coastal amenity and the convex decline in flooding disamenity as we move away from the coast, with the marginal effect of both equating at the CBD. The figure also shows commuting costs rising in distance to the CBD. Finally, the bottom panel shows the housing density and the city boundaries.

In Fig. 5 we report some of our findings from the simulations, focusing on the extensive margins of city expansion, corresponding to our initial question: where do people build on LECZ?

We initially consider the baseline simulation, with no sea level rise. This scenario, which is described in panel (a) of Fig. 5, illustrates some of the empirical findings that we discuss above: in 1990 the city is relatively small, and hence only slightly asymmetric around its CBD. As the city becomes bigger, it also becomes more asymmetric. The city expands on both sides, and the expansion on the coast-side is towards increasingly flood-prone areas, taking in the least-bad locations that are still unbuilt. Panel (b) shows estimates from the dynamic equivalent of this scenario, and the results are largely unchanged.

Next, we add baseline sea level rise in panel (c) of Fig. 5, using the midway point between the two main scenarios in Pörtner et al. (2019), for a city whose elevation is similar to Miami's, with a CBD 2 meters above sea level. Now we can see that the city's advance on the coast side is slower, even without dynamic considerations, because locations close to the coast become increasingly flood-prone even before they are submerged. Nevertheless, the city expands towards the coast, even taking in locations that are later submerged. In this case switching land use and even an abandonment of part of the city is (by assumption) not directly costly, but SLR still distorts the city, by making it more asymmetric. Another aspect of this distortion is the more rapid expansion of the city on the inland side, where the marginal benefit of the approaching coast is, at least for a while, positive, as can be seen from the city founder's problem. The combined effect of the slower expansion on the coast side and the more rapid expansion on the inland side further distorts the city's shape and lengthens typical commutes.[37] Finally, we observe a small area of the city where the number of housing units declines by more than 10 percent relative to the peak density across all previous periods.[38] In the model this does not cause problems to anyone other than the developer. But in reality, neighborhoods with declining demand may lead to a host of economic and social problems, although these lie outside the scope of our model.

In the dynamic version that corresponds to this scenario (Panel (d)), the city expands less on the coast side, as the cost of development deters some of the expansion in the face of SLR. On the inland side, however, the expansion is very similar to the static model with moderate SLR.

In Panel (e) we consider the case of rapid SLR – 1.5 times the speed of the baseline SLR. This faster speed may represent one of the three factors: faster local SLR on the US Atlantic and Gulf coast than the global mean, as discussed above; a city with a lower elevation CBD, of about 1.33 m; or moderately faster global SLR than currently anticipated. Even in this case the city expands towards the coast as the coast moves closer to the city, resulting in higher costs of flooding. The coast-side expansion is, however, slower in this case, and stops altogether in the dynamic version of this scenario (Panel f). In this case, especially in the dynamic model where urban land cannot be reconverted into agricultural land, there are even more declining neighborhoods. At the same time, in both Panels (e) and (f) the city expands even more on the inland side, because the faster-moving coastline brings the inland locations closer to the coast, increasing their amenity value (net of flood costs), at least for a while. This results in a further distortion of the city's shape, and even longer commutes. Finally, the fast SLR scenario highlights the problem that the city ultimately faces: to survive SLR in the long run, it needs to move its CBD, which could be very costly, and again lies outside the scope of the model.

In Appendix Figure A10 we consider additional scenarios. The first two panels show a city without rising wages, but with rapid SLR. Here the city shrinks due to SLR, with the coast-side contraction more sizeable than the inland-side expansion. In the static case (Panel (a)), urban land is converted to agriculture on the coast-side as the coast approaches, while in the dynamic case (Panel (b)) those neighborhoods go into decline. The next two panels of Figure A10 consider a government

[36] In recent and related work Ospital (2023) studies the effects of excessive regulation on wildfire risk in California.

[37] The existence of multiple employment centers within the city, which we do not model, may mitigate some of the distortion caused by longer commutes.

[38] Using the 10 percent threshold allows us to visualize economically declining locations. The demand-driven declines, caused by rising flood risk, represent a larger fall in period prices than 10 percent, and with SLR these locations eventually become uninhabitable.

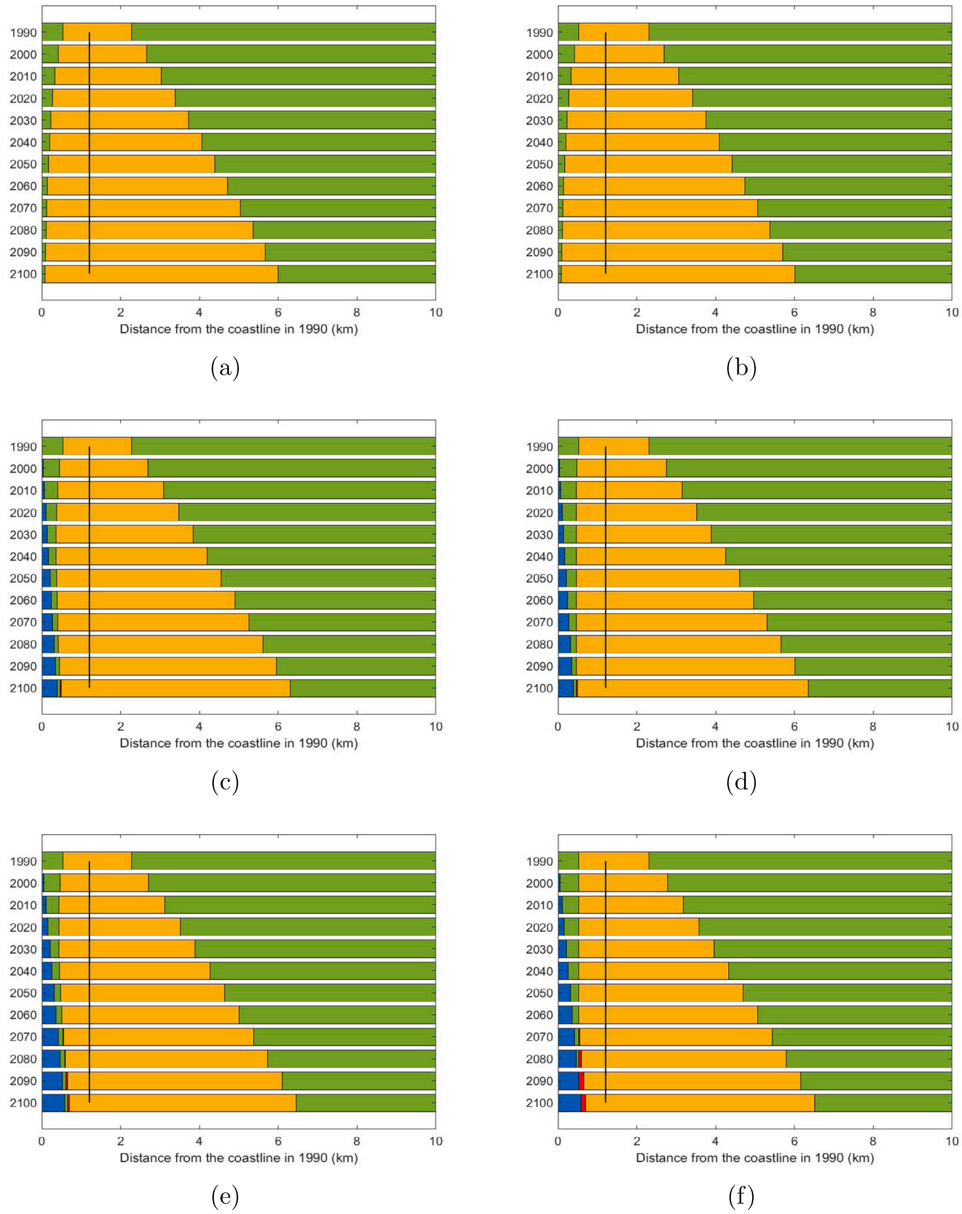

Fig. 5. The figure shows results of simulations, as described in the main text, and based on parameter values detailed in Table A8. Panel (a) shows results from the static model with no SLR. Panel (b) is the same but for the dynamic version of the model. Panel (c) shows results from the static model with baseline SLR (0.0577 m per decade, CBD at 2 m elevation). Panel (d) shows the same for the dynamic model. Finally, panel (e) shows results from the static model with faster SLR (equivalent to a city with CBD at 1.33 m elevation), and Panel (f) the equivalent results for the dynamic model. In the figure yellow denotes the city, green denotes agricultural land, blue denotes the sea, and red denotes areas whose housing density declined at least 10 percent from the maximum level. The time period is on the vertical axis in 10 year time-steps, and the horizontal axis shows distance to the coast in km.

subsidy to offset some of the flood costs with baseline SLR. In the static case (Panel (c)), this leads to faster expansion on the land side in the face of SLR, and even in the dynamic case (d), we see rapid expansion towards the coast, in contrast to the case without subsidy, as discussed above.

The bottom two panels of Figure A10, (e) and (f), consider the case with an alternative commuting elasticity of 0.0729 as per Duranton and Puga (2019). This lower elasticity accounts for the presence of multiple employment locations within the city, reflecting the idea that people may find jobs in various areas beyond the CBD and do not always have to commute to the center. Here the city expands more than in the baseline, although the cost of this expansion is lower since people's commutes are shorter.

In addition to the scenarios above, we also considered the case where the CBD location is not chosen just once by the city founder but is selected in each period to trade off the amenity and disamenity of coastal proximity (results available on request). In this case, the CBD and housing gradually shift inland as sea levels rise. This allows cities to overcome the problem of SLR in the static case, or mitigate them considerably in the dynamic case, where left-behind declining neighborhoods are now also further from the CBD, and new extensive-margin developments are costly. This version of the model, however, does not account for the costs of building new buildings to replace existing ones, and the coordination costs involved in moving a CBD.[39]

[39] Alternatively, we also explored the case where the CBD is immobile but located at the empirical peak of the housing density instead of the model-predicted location. This leads at least in the short run, to cities skewed around their CBD in the opposite way to what we observe in the data, since locational

Finally, Figure A11 considers the case of a closed city with restrictive regulation. In Panel (a) we simulate decadal population growth of 5%, without a greenbelt restriction, and in panel (b) we add a green belt extending inland from the 1990 inland edge of the city. Panels (c) and (d) repeat the analysis with a decadal population growth of 10%. In both cases, the green belt pushes population further into the flood-prone area near the coast.

In summary, these simulations highlight four problems of low-elevation cities. First, the problem of flooding worsens over time, either because cities expand towards the coast, or because of SLR, or because both happen simultaneously. This development threatens to increase flooding costs for both residents and taxpayers. The costs could be exacerbated by government subsidies to flood-prone areas. Second, even if LECZ cities grow on aggregate, some neighborhoods decline, as increased flood risk causes prices and population to decline. This problem is worse for cities that are economically stagnant. Third, SLR further distorts the shape of LECZ cities, significantly lengthening the time costs of commuting to work. Finally, LECZ cities face a potential crisis if their CBD comes under threat of being permanently submerged, so it is important to consider how moveable this center of economic activity is, and at what cost.

4.5.3. Welfare analysis

The main rationale for the model is to provide a parsimonious explanation for the stylized facts and auxiliary findings, and qualitatively explore different scenarios, as we do above. Our model considers a relatively benign case, where people correctly anticipate events, and the city adapts gradually. Further, the model does not consider idiosyncratic conditions that specific cities may face. We also note that time discounting crucially affects all our estimates, and in many cases the losses increase over time. With these caveats in mind, we cautiously proceed to explore some of the model's welfare implications. We note that in the model residents' utility is fixed, so we measure welfare using the value of landowners' land, net of any transfers.

In Columns (1) and (2) of Appendix Table A9, we compute the percentage changes in the present discounted value of land, between the scenario without SLR and each of the two SLR scenarios (baseline and fast SLR). In the city as a whole, the losses from SLR are around 1.5–2.4 percentage points, with higher losses with fast SLR and in the dynamic case. Land within 1 km from the coast, however, bears the brunt of these losses, falling in value by around 20–30 percent due to SLR. The intuition for this result is that SLR submerges land near the coast and changes the payoffs for inland locations, so those near the coast lose out, while those further inland (where the marginal coastal amenity is higher than its marginal disamenity) may gain, at least as long as they are not submerged.

We next consider the economic loss from government subsidies, which encourage the city's (over) expansion, especially the coastal side. Column (3) of Table A9 shows that even without SLR, the net loss from subsidies in the city as a whole is around 1 percent in the static and 2 percent in the dynamic case. The loss from the subsidy is again unevenly distributed, concentrating mostly in the 1 km near the coast, where it is around 6–7.5 percentage points. Columns (4) and (5) show a similar loss from the subsidy with SLR, since the city adjusts by expanding inland. We note, however, that this loss comes on top of the loss from SLR itself, as discussed above. As discussed above, the model does not account for risk aversion and the role of flood insurance that may be difficult to obtain privately. At the same time, we note that the ratio of the subsidy to (land values without subsidy) is higher than the welfare loss, amounting to 5.3–6.4 percent for the city as a whole and 15–20 percent within 1 km of the coast, most of which is capitalized into land values.

fundamentals and CBD location attract population to two different locations. We therefore do not consider this case to be of much empirical relevance.

Finally, we examine the role of an immobile (path dependent) CBD, which affects the city's shape and the commuting cost. In Columns (6) and (7) of Table A9, we report the percentage change in cumulative land value in the model where the CBD is fixed in the first period relative to a model where the CBD adjusts costlessly each period. The loss here (0.16–0.25 percentage points) is small compared to the previous cases. An important caveat to this finding is that it considers only cases where the CBD is not inundated by SLR.

4.5.4. Policy implications

Governments could enact various policies to mitigate the problems discussed above. First, to limit taxpayer exposure, governments could consider taxing new developments in flood-prone areas, if there are viable alternative uses to the land, which are not taxed. The difference between the dynamic scenarios (where extensive margin adjustments are costly) and the static scenarios suggest that with SLR, raising the costs of extensive margin development restricts it to some extent.

Second, governments could offer the subsidy only to existing housing. One such policy is the UK government's Flood Re, which provides subsidized flood insurance only to "grandfathered" housing, built before 2009 (see https://www.floodre.co.uk/can-flood-re-help-me/eligibility-criteria/). Comparing the outcomes in Panels (c) and (d) of Fig. 5 (without a subsidy) with Panels (c) and (d) of Figure A9 (with a subsidy), we see that the subsidy led to more coast-side expansion, so withdrawing it could help limit government exposure.

Third, if withdrawing subsidies is unfeasible, governments could attach further conditions to their subsidy. These conditions could include stricter building standards, such as construction on stilts imposed by the US Federal government when compensating the victims of Hurricane Sandy (e.g., https://www.ft.com/content/f95aa4e2-b3e6-11e7-aa26-bb002965bce8). Or governments could restrict the number of times a given property is bailed out, or offer other incentives to move instead of rebuilding, as Canada has recently done (e.g., https://www.nytimes.com/2019/09/10/climate/canada-flood-homes-buyout.html). With SLR proceeding at pace, the costs to taxpayers of fixing neighborhoods or even cities may at some point become prohibitive. An example of how far things have deteriorated in another part of the world can be seen in Indonesia, whose government is investing heavily in moving its capital from flood-prone Jakarta (e.g., https://www.ft.com/content/5a463614-c7e4-11e9-af46-b09e8bfe60c0)

Ultimately, of course, slowing down climate change and SLR could also reduce the costs, especially those associated with large-scale urban moves. This remains a central policy challenge.

5. Conclusions

This paper contributes to our understanding of housing construction in LECZ. We begin by documenting two stylized facts and four auxiliary findings. These reveal the distribution of housing stock density, which peaks near the coast. They also show the asymmetry of the housing density distribution and of places near the coast, an asymmetry which is particularly pronounced for large places. We relate these findings to the tradeoff between the amenity value of proximity to the coast, conditional on flood-proneness. We show how new construction in recent decades avoided flood-prone areas in sparse locations, but in dense locations new construction took place on the least-bad flood-prone areas.

We then develop a simple model of a monocentric city, which combines the amenity value of proximity to the coast with a convex cost of building very close to the coast. This model allows us to explain the patterns that we see, and answer questions such as: why does population concentrate near (but not right at) the coast? Why are coastal places asymmetric? Why does this asymmetry vary by place size? And why does construction take place in flood-prone urban fringes?

Finally, we extend our model and use it to study how SLR may reshape cities. This allows us to explore the evolution of future flood costs, as cities expand towards the coast even as the coast moves towards them; the economic decline of areas even within expanding cities, as SLR reduces demand for locations that become increasingly flood-prone; the lengthening of commutes, as cities' asymmetry around their historical CBDs grows; and the threats to coastal cities that depend on low-elevation CBDs.

By combining empirical evidence with a simple and highly adaptable model, our paper offers a path for researchers and policy makers to consider the implications of a range of interventions in low-elevation coastal cities, in an era when climate change poses increasingly important challenges.

CRediT authorship contribution statement

Yatang Lin: Writing – review & editing, Writing – original draft, Visualization, Validation, Supervision, Software, Resources, Project administration, Methodology, Investigation, Funding acquisition, Formal analysis, Data curation, Conceptualization. **Thomas K.J. McDermott:** Writing – review & editing, Writing – original draft, Visualization, Validation, Supervision, Software, Resources, Project administration, Methodology, Investigation, Funding acquisition, Formal analysis, Data curation, Conceptualization. **Guy Michaels:** Writing – review & editing, Writing – original draft, Visualization, Validation, Supervision, Software, Resources, Project administration, Methodology, Investigation, Funding acquisition, Formal analysis, Data curation, Conceptualization.

Data availability

https://data.mendeley.com/datasets/2jrct63w2t/2.

Appendix A. Supplementary data

Supplementary material related to this article can be found online at https://doi.org/10.1016/j.jue.2024.103685.

References

Alonso, William, 1964. Location and Land Use. Toward a General Theory of Land Rent. In: Publication of the Joint Center for Urban Studies, Harvard University Press, Cambridge, MA.
Bakkensen, Laura A., Barrage, Lint, 2021. Going underwater? Flood risk belief heterogeneity and coastal home price dynamics. Rev. Financ. Stud..
Balboni, Clare, 2020. In Harm's way? Infrastructure investments and the persistence of coastal cities revise & resubmit. Amer. Econ. Rev..
Barrage, Lint, Furst, Jacob, 2019. Housing investment, sea level rise, and climate change beliefs. Econom. Lett. 177, 105–108.
Beltran, A., Maddison, D., Elliott, R., 2018. Is flood risk capitalised into property values? Ecol. Econ. 146, 668–685.
Berardelli, Jeff, 2019. How Climate Change Is Making Hurricanes More Dangerous. Yale Climate Connections. CT, New Haven, Accessed July 2020 at https://yaleclimateconnections.org/2019/07/how-climate-change-is-making-hurricanes-more-dangerous/.
Bester, C. Alan, Conley, Timothy G., Hansen, Christian B., 2011. Inference with dependent data using cluster covariance estimators. J. Econometrics 165 (2), 137–151.
Bleakley, Hoyt, Lin, Jeffrey, 2012. Portage and path dependence. Q. J. Econ. 127 (2), 587–644.
Brody, S.D., Zahran, S., Maghelal, P., Grover, H., Highfield, W.E., 2007. The rising costs of floods: Examining the impact of planning and development decisions on property damage in Florida. J. Am. Plan. Assoc. 73 (3), 330–345.
Burby, Raymond J., 2001. Flood insurance and floodplain management: The US experience. Environ. Hazards 3 (3), 111–122.
Burningham, Kate, Fielding, Jane, Thrush, Diana, 2008. 'It'll never happen to me': Understanding public awareness of local flood risk. Disasters 32 (2), 216–238.
Conley, Timothy G., 1999. GMM estimation with cross sectional dependence. J. Econometrics 92 (1), 1–45.
Dahl, Kristina A., Fitzpatrick, Melanie F., Spanger-Siegfried, Erika, 2017. Sea level rise drives increased tidal flooding frequency at tide gauges along the U.S. East and Gulf Coasts: Projections for 2030 and 2045. PLoS One 12 (2).
Database of Global Administrative Boundaries (GADM), 2018. USA country outline (version 3.6). Davis, CA: GADM. Accessed September 2020 at https://gadm.org/download_country_v3.html.
Deryugina, Tatyana, 2017. The fiscal cost of hurricanes: Disaster aid versus social insurance. Am. Econ. J.: Econ. Policy 9 (3), 168–198.
Desmet, Klaus, Kopp, Robert E., Kulp, Scott A., Nagy, Dávid K., Oppenheimer, Michael, Rossi-Hansberg, Esteban, Strauss, Benjamin H., 2021. Evaluating the economic cost of coastal flooding. Am. Econ. J.: Marcoecon..
Dinan, Terry, 2017. Projected increases in hurricane damage in the United States: The role of climate change and coastal development. Ecol. Econ. 138, 186–198.
Donaldson, Dave, Hornbeck, Richard, 2016. Railroads and American economic growth: A market access approach. Q. J. Econ. 131 (2), 799–858.
Duranton, Gilles, Puga, Diego, 2014. In: Aghion, Philippe, Durlauf, Steven N. (Eds.), Chapter 5 - The Growth of Cities in Handbook of Economic Growth, vol. 2, pp. 781–853.
Duranton, Gilles, Puga, Diego, 2019. Urban growth and its aggregate implications. NBER Working Paper 26591.
Federal Reserve Bank of St. Louis, 2020. Gross Domestic Product: Implicit Price Deflator (GDPDEF). Federal Reserve Bank of St. Louis, St. Louis, MO, Accessed January 2021 at https://fred.stlouisfed.org/series/GDPDEF.
Gibson, Matthew, Mullins, Jamie T., 2020. Climate risk and beliefs in New York floodplains. J. Assoc. Environ. Resource Economists 7 (6), 1069–1111.
Glaeser, Edward L., Kolko, Jed, Saiz, Albert, 2001. Consumer city. J. Econ. Geography 1 (1), 27–50, Oxford University Press.
Gyourko, J., Hartley, J., Krimmel, J., 2019. The Local Residential Land Use Regulatory Environment Across U.S. Housing Markets: Evidence from a New Wharton Index. National Bureau of Economic Research wp 26573.
Harari, Mariaflavia, 2020. Cities in bad shape: Urban geometry in India. Amer. Econ. Rev. 110 (8), 2377–2421.
Henderson, J. Vernon, Regan, Tanner, Venable, Anthony J., 2020. Building the city: From slums to a modern Metropolis. Rev. Econ. Stud. 88 (3), 1157–1192.
Hino, M., Burke, Marshall, 2020. Does information about climate risk affect property values? NBER Working Paper, no. 26807.
Hornbeck, Richard, Keniston, Daniel, 2017. Creative destruction: Barriers to urban growth and the great boston fire of 1872. Amer. Econ. Rev. 107 (6), 1365–1398.
Keys, Benjamin J., Mulder, Philip, 2020. Neglected no more: Housing markets, mortgage lending, and sea level rise. NBER Working Paper, no. 27930.
Kocornik-Mina, Adriana, McDermott, Thomas, Michaels, Guy, Rauch, Ferdinand, 2020. Flooded cities. Am. Econ. J.: Appl. Econ. 12 (2), 35–66.
Kousky, C., Michel-Kerjan, E., 2017. Examining flood insurance claims in the United States: Six key findings. J. Risk Insur. 84 (3), 819–850.
Kousky, Carolyn, Olmstead, Sheila M., Walls, Margaret A., Macauley, Molly, 2013. Strategically placing green infrastructure: Cost-effective land conservation in the floodplain. Environ. Sci. Technol. 47 (8), 3563–3570.
Kriesel, W., Landry, C., 2004. Participation in the National Flood Insurance Program: An empirical analysis for coastal properties. J. Risk Insur. 71 (3), 405–420.
Kydland, Finn E., Prescott, Edward C., 1977. Rules rather than discretion: The inconsistency of optimal plans. J. Polit. Econ. 85 (3), 473–491.
Magontier, Pierre, Solé-Ollé, Albert, Viladecans-Marsal, Elisabet, 2019. The political economy of coastal destruction. Mimeo.
Manson, Steven, Schroeder, Jonathan, Riper, David Van, Ruggles, Steven, 2019. IPUMS National Historical Geographic Information System: Version 14.0 [Database]. IPUMS, Minneapolis, MN, http://dx.doi.org/10.18128/D050.V14.0, Accessed February 2021 at.
Marcy, Doug, Herold, Nate, Waters, Kirk, Brooks, William, Hadley, Brian, Pendleton, Matt, Schmid, Keil, Sutherland, Mike, Dragonov, Kyle, McCombs, John, Ryan, Sean, 2011. New Mapping Tool and Techniques for Visualizing Sea Level Rise and Coastal Flooding Impacts. NOAA Coastal Services Center, Charleston, SC, Accessed September 2020 at https://coast.noaa.gov/data/digitalcoast/pdf/slr-new-mapping-tool.pdf, originally published in the Proceedings of the 2011 Solutions to Coastal Disasters Conference, American Society of Civil Engineers (ASCE), and reprinted with permission of ASCE.
Michel-Kerjan, E.O., 2010. Catastrophe economics: the national flood insurance program. J. Econ. Perspect. 24 (4), 165–186.
Mills, Edwin S., 1967. An aggregative model of resource allocation in a metropolitan area. Am. Econ. Rev. Pap. Proc. 57 (2), 197–210.
Muth, Richard F., 1969. Cities and Housing. University of Chicago Press, Chicago.
National Oceanic and Atmospheric Administration (NOAA), 2021a. Billion-Dollar Weather and Climate Disasters: Summary Stats. NOAA, Washington DC, (2021) Accessed February 2021 at https://www.ncdc.noaa.gov/billions/summary-stats/US/2005-2020.
National Oceanic and Atmospheric Administration (NOAA), 2021b. Sea Level Rise Viewer. NOAA, Washington DC, (2021) Accessed June 2020 at https://coast.noaa.gov/digitalcoast/tools/slr.html.
National Oceanic and Atmospheric Administration (NOAA), 2021c. Digital Coast. NOAA, Washington DC, (2021) Accessed June 2020 at https://coast.noaa.gov/digitalcoast/data/.
Neumann, Barbara, Vafeidis, Athanasios T., Zimmermann, Juliane, Nicholls, Robert J., 2015. Future Coastal population growth and exposure to sea-level rise and coastal flooding - A global assessment. PLoS One 10 (3).
Ortega, F., Taşpınar, Süleyman, 2018. Rising sea levels and sinking property values: Hurricane Sandy and New York's housing market. J. Urban Econ. 106, 81–100.
Ospital, A., 2023. Urban policy and spatial exposure to environmental risk. Mimeo.

Peter G. Peterson Foundation, 2020. Budget basics: The national flood insurance program. Accessed March 2021 at: https://www.pgpf.org/budget-basics/the-national-flood-insurance-program.

Pörtner, Hans O., Roberts, Debra C., Masson-Delmotte, Valérie, Zhai, Panmao, Tignor, Melinda, Poloczanska, Elvira, Mintenbeck, Katja, Alegría, Andrés, Nicolai, Maike, Okem, Andrew, Petzold, Jan, Rama, Bardhyl, Weyer, Nora M., 2019. IPCC Special Report on the Ocean and Cryosphere in a Changing Climate. United National Inter-Governmental Panel on Climate Change, Geneva, Switzerland.

Pralle, S., 2019. Drawing lines: FEMA and the politics of mapping flood zones. Clim. Change 152, 227–237.

Pryce, Gwilym, Chen, Yu, Galster, George, 2011. The impact of floods on house prices: An imperfect information approach with myopia and amnesia. Housing Stud. 26 (2), 259–279.

Rappaport, J., 2007. Moving to nice weather. Reg. Sci. Urban Econ..

Rappaport, J., Sachs, Jeffrey D., 2003. The United States as a coastal nation. J. Econ. Growth 8 (1), 5–46.

Saiz, Albert, 2010. The geographic determinants of housing supply. Q. J. Econ. 125 (3), 1253–1296.

Taylor, C.A., Druckenmiller, H., 2022. Wetlands, flooding, and the clean water act. Amer. Econ. Rev. 112 (4), 1334–1363.

U.S. Congressional Budget Office (CBO), 2017. The national flood insurance program: Financial soundness and affordability. available online from www.cbo.gov/publication/53028.

U.S. Congressional Budget Office (CBO), 2019. Expected Costs of Damage from Hurricane Winds and Storm Related Flooding. Congressional Budget Office, Washington DC, Accessed July 2020 at: https://www.cbo.gov/system/files/2019-04/55019-ExpectedCostsFromWindStorm.pdf.

US Department of Homeland Security, Office of Inspector General, 2017. FEMA needs to improve management of its flood mapping programs. Report for office of the inspector general. OIG-17-110.

Wing, O.E., Bates, P.D., Smith, A.M., Sampson, C.C., Johnson, K.A., Fargione, J., Morefield, P., 2018. Estimates of present and future flood risk in the conterminous United States. Environ. Res. Lett. 13 (3).